

Chapter 4

Up-Conversion

Luminescence Study

Introduction

In the general process of luminescence, a lower energy photon is generated on excitation by a higher energy photon. However, in the case of upconversion, the process is exactly the opposite. i.e. higher energy photons are generated on excitation by multiple low energy photons. Generally, two electrons of lower energy, in near infrared region carry out the excitation process by subsequent absorption. The emission process is a single step process by radiative energy transfer and results in a photon in the visible region. The process is different than the simultaneous multi photon absorption in the sense that the intermediate level is virtual, while in case of up conversion, it is real. This results into higher efficiency in case of upconversion process, which leads to several applications [1].

The process of photon, upconversion has been extensively studied in particularly lanthanide-doped materials. These studies have opened up a large number of potential applications like infrared pumped visible lasers, colour display, optical storage, solar cells and bio-labels. The lanthanides have been particularly useful in the field of up conversion due to their rich energy levels and long lived excited states, which result from the unique electron configuration of these elements i.e. the f-block elements, whose electrons in the 4f shells are effectively shielded by 5s and 5p shells, which are in close proximity. The shielding ensures that there is hardly any perturbation due to the local environment of the host lattice, leading to steady spectroscopic properties i.e. the exhibition of sharp emission bands almost independent of the host lattice. The sharp emission bands leads to better colour characteristics in terms of purity of colour, as they can be doped in various solid matrices while retaining the same colour characteristics [2]. In case

of multiphoton processes, a handful of trivalent rare earth ions serve as the absorption and emission centers. They are Yb, Er, Sm, Ho, Pr and Tm (Ytterbium, Erbium, Samarium, Holmium, Promethium and Thulium)

4.1 Mechanism of up conversion

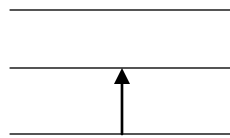
The mechanism of up conversion has the usual two step process.

- a. Absorption
- b. Energy transfer (non-radiative)

“The process of absorption” can be categorized into two:

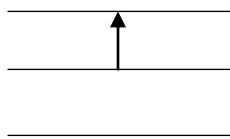
- (i) Ground State Absorption (GSA)

Here, an ion in the ground state absorbs energy to go the excited state



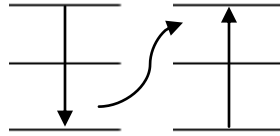
- (ii) Excited State absorption (ESA)

Here, an ion in the excited state absorbs energy and goes to a higher excited state.

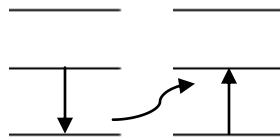


The process of Energy transfer can be categorized as under.

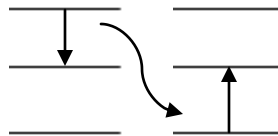
- (i) Energy transfer between the same kind of ions, which is a very common form of energy transfer.



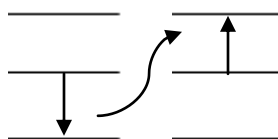
- (ii) “Energy Transfer” between different kind of ions. It happens for a pair of ions, one acting as activator and other sensitizer.



- (iii) Energy released by an ion to come from a higher excited state to a lower excited state is absorbed by another ion to move from ground state to lower excited state. Hence both the ions are in lower excited state. This is called “Cross Relaxation”(CR)



- (iv) Energy released by an ion in the lower excited to come down to the ground state is absorbed by an ion in the lower excited state to go the higher excited state. This is called “Energy Transfer Upconversion (ETU)”.



A combination of the above processes make up for the complete process of upconversion.

1. Ground State Absorption is followed by Excited State Absorption. (GSA/ ESA)

This process is inherent in case of materials with single optical center. Hence it is relatively insensitive to the concentration of the optical center i.e. the ion which produces up conversion.

2. Ground State Absorption is followed by Energy transfer up-conversion (GSA/ ETU)

This process is inherent in case of materials with two optical centers i.e. one activator and one sensitizer. Initially the ions are activated by ground state absorption, which is followed by energy transfer up-conversion. This is the most common up-conversion mechanism. The advantage with such up-conversion processes is that they require a low power source e.g. low power continuous wave diode laser. [3]

The phenomenon of up conversion was put forward way back in 1959. It was called the “Quantum counter action”, which in today’s context, is known as the “Excited state absorption”. Right from the initial stage, it was observed in rare earth activate materials. Subsequent studies have established that the effectiveness of the up conversion mechanism depends on the

- Host material
- Activator
- Sensitizer
- Concentration of activator and sensitizer

The efficiency of up conversion is dependent on

- the spatial distribution of dopant ions
- the structure of host lattice

The dopant concentration and the structure of host lattice must be such that it leads to the enhancement in the formulation of complexes of associated ions. If this condition is fulfilled, the up-conversion efficiency increases.

4.2 Electronic structure of Lanthanide elements

The Lanthanide group in the periodic table consists of 15 elements.

Element	Atomic Number
Lanthanum	57
Cerium	58
Praseodymium	59
Neodymium	60
Promethium	61
Samarium	62
Europium	63
Gadolinium	64
Terbium	65
Dysprosium	66
Holmium	67

Erbium	68
Thulium	69
Ytterbium	70
Lutetium	71

The elements Yttrium (39) and Scandium (21) are also considered to be associated with the lanthanide group.

The electronic configuration of the rare earth (Lanthanide) atoms are built up as

Xe Core

(1s², 2s², 2p⁶, 3s², 3p⁶, 4s², 3d¹⁰, 4p⁶, 5s², 4d¹⁰, 5p⁸)

+

2 or 3 outer electrons (6s² or 6s² 5d¹)

and

4f electrons (0 to 14)

The successive elements in the group have incremental filling of electrons in the 4f shell from 4f⁰ in Lanthanum to 4f¹⁴ in Lutetium. By losing the 6s and 5d electrons, they are generally available in the trivalent ionic state. However, the 5s and 5p electrons shield the 4f electrons, making them almost insensitive to the surrounding environment. Since the up-conversion process involves 4f - 4f transitions, the absorption and emission cross sections are very small, while the Luminescence life times are relatively long (up to few milli seconds) [4]

The Lanthanide elements, in general, are considered to be non-toxic and having unique emission properties in a wide range of wavelengths from ultraviolet to near infrared, resulting into their potential applications in lasers, lighting and optical fiber. Lanthanide ions are widely used as activators in solid-state lasers, lamps, displays, communication systems and other photonic devices. [4]

The Lanthanide elements have the same valence electrons. Hence, the ions show similar behavior in terms of coordination and reactivity. The Luminescence properties of these ions, which are mostly in the trivalent state, arise from transitions within the 4f shell. Due to the shielding effect, their absorption and emission characteristics remain almost the same in any host lattice. [4]

The transitions that give Luminescence are in accordance with the Russel Saunders or LS coupling scheme. In case of LS coupling, the formula by which each of these levels are labelled is given by

$$^{2S+1}L_J$$

where S corresponds to the total spin multiplicity,

L is the orbital angular momentum and J represents total angular momentum.

Energy level diagrams of the Lanthanide ions, based on such schemes are widely available. They are valid for these ions incorporated in different host lattices, as the shielding effect ensures that there is no appreciable change due to the local fields. These diagrams do not generally include the Lanthanum (La^{3+}) and Lutetium (Lu^{3+}) ions as the former has empty while the latter has a completely filled 4f shell.

Both electric as well as magnetic dipole transitions are allowed within the 4f states, with some exception, as the symmetry of the environment influences the selection rules of these transitions. Electric dipole transitions are not allowed in a crystal site with inversion symmetry. However, if the ion is under the influence of a non-center symmetric crystal field, the selection rule relax to partly allow such transitions. Such transitions are termed, induced electric dipole transitions. [5] In such cases, the interactions lead to the mixing of higher energy configurations of opposite parity into the 4f wave functions through the odd terms of the crystal field potential. [6]

Magnetic dipole transitions are readily allowed. However, they are weak. Both types of transitions have similar intensities in the trivalent ion spectra, as one is weak and the other happens as a consequence of a perturbation. [3]

4.3 Up conversion in Erbium (Er^{3+})

Very few ions have the ability to exhibit up conversion luminescence as an activator or sensitizer. While Erbium, Holmium, Praseodymium and Thulium are the only elements, which act as an activator, the role of synthesizer is limited to Ytterbium and Samarium. Erbium can be both an activator and sensitizer.

Erbium in its tri-positive state (Er^{3+}) is one of the most efficient ions for up conversion, for the following reasons:

- Existence of metastable levels $^4I_{11/2}$ and $^4I_{9/2}$ corresponding to 973 nm and 800nm respectively, apart from other levels.

- Has a favorable electronic energy level scheme with equally spaced long lived excited states.

Hence, Erbium has been studied as an activator in several materials. A couple of illustrations are mentioned below.

Erbium doped KLaF₄, when excited by 980nm radiation exhibits emission features as narrow band spectra with a dominant peak at 522 nm corresponding to the transition $^2H_{11/2} \rightarrow ^4I_{15/2}$ and smaller peaks at 545nm and 660nm corresponding to $^4S_{3/2} \rightarrow ^4I_{15/2}$ respectively [7]. It is used for 2D and 3D assemblies and in bioprobes.

In Bi₂Ti₄NbO₂₁ ceramics, the excitation of 980 nm gives emission peaks at 533 nm, 550 nm and 670 nm for the transitions $^2H_{11/2} \rightarrow ^4I_{15/2}$, $^4S_{3/2} \rightarrow ^4I_{15/2}$ and $^4F_{9/2} \rightarrow ^4I_{15/2}$ respectively. The peak at 550 nm has the highest intensity. The material finds use in optical thermometry, electro-optical devices and bio imaging. [8]

Erbium doped CeO₂ and SiTiO₃ have been investigated for excitation at 785 nm [9, 10]

BaCl₂: Er³⁺ has been studied for multiple excitations of 800nm, 970 nm and 1500 nm [11].

However, there are limitations in using Erbium as a single dopant in terms of up conversion efficiency. Attempts at increasing the efficiency by increasing dopant concentration have failed. This is because, at higher concentrations, the Er³⁺ ions indulge in cross relaxation, resulting into quenching of emission. Another limitation is that in Erbium ions, the absorption cross section for

the transition around 980 nm is relatively low, about $1.7 \times 10^{-21} \text{ cm}^2$ at 976 nm, to be precise. These limitations lead to poor emission efficiency.

4.4 Up conversion in Erbium (Er^{3+}) with Ytterbium (Yb^{3+})

The efficiency can be increased by adding a sensitizer or co-activator along with Er^{3+} , which has a better absorption cross section. The role of such a sensitizer can be accomplished by Ytterbium (Yb^{3+}), which has a much higher absorption cross section of about $11.7 \times 10^{-21} \text{ cm}^2$ at 976 nm. Hence the Yb^{3+} ion can efficiently absorb the radiation and transfer it to Er^{3+} . The spectral states for Yb^{3+} emission, $^2\text{F}_{5/2} \rightarrow ^2\text{F}_{7/2}$ and Er^{3+} absorption, $^4\text{I}_{11/2} \rightarrow ^4\text{I}_{15/2}$ are almost at the same energy level causing a large spectral overlap between them that results into efficient energy transfer and subsequently improves the emission efficiency significantly. [12]

The simple two level system of Yb^{3+} helps in ensuring that even at high concentrations, there is no quenching as part of the energy is transferred to Er^{3+} . Besides, the ionic radius of Yb^{3+} and Er^{3+} ions are similar. This enables suitable incorporation of these two ions in the host matrices. [13]. The presence of Yb^{3+} as sensitizer induces donor-acceptor processes between Er^{3+} and itself. Thus, the combination of Er^{3+} and Yb^{3+} yields good results in particularly low phonon energy host matrices.

Along with efficiency of up conversion, another important factor is the spectral characteristics of emission. The choice of host matrix is important here as the emission characteristics can be manipulated by control of host/ dopant combinations, apart from dopant concentration [14].

A practical problem arises due to the sharp absorption and emission lines of lanthanide doped phosphors, which typically have 10 – 20 nm full width at half maximum. This imposes constraints on the selection of the excitation source. However, this problem is solved due to the availability of InGaAs diode laser system operating at 980nm, which matches with the absorption of Yb^{3+} ions.

The host matrices chosen for the study have not been studied extensively but hold a lot of potential in terms of efficiency and spectral characteristics. Lanthanum Molybdate doped with Erbium and Ytterbium [$\text{La}_2(\text{MoO}_4)_3:\text{Er}^{3+}/\text{Yb}^{3+}$], Bismuth Oxide doped with Erbium and Ytterbium [$\text{Bi}_2\text{O}_3:\text{Er}^{3+}/\text{Yb}^{3+}$] and Cadmium Oxide doped with Erbium and Ytterbium [$\text{CdO}:\text{Er}^{3+}/\text{Yb}^{3+}$], in their limited exploration so far, have shown strong emission characteristics.

In an earlier work, $\text{La}_2(\text{MoO}_4)_3:\text{Er}^{3+}/\text{Yb}^{3+}$ particles prepared by microwave-modified sol-gel method, under the excitation of 980 nm, exhibited strong emission at 525 nm, 550 nm and 655 nm for ${}^2\text{H}_{11/2} \rightarrow {}^4\text{I}_{15/2}$, ${}^4\text{S}_{3/2} \rightarrow {}^4\text{I}_{15/2}$ and ${}^4\text{F}_{9/2} \rightarrow {}^4\text{I}_{15/2}$ transitions of Er^{3+} ions respectively. [15]

Similarly, Bi_2O_3 prepared through a solid-state-chemistry thermal decomposition process exhibits intense upconversion luminescence on doping Yb, Er ions into the host matrix under 980 nm excitation. It has been utilized for temperature sensing and optical imaging applications [16].

CdO has not been explored for up-conversion characteristics so far.

4.5 Up-conversion phosphor applications

Up-conversion materials are useful due to their applications which follow from their characteristics to convert infra red into visible light. Some of the prominent ones are mentioned below.

There are many luminescent materials, which give visible light on excitation by ultraviolet radiation. These materials have been conventionally used for lighting applications. There are materials, which emit in the infrared region when excited by electric field. This infrared component can be converted into visible light using up-conversion phosphors. Such materials, along with up-conversion phosphors are used for Light Emitting Diodes.

These phosphors, particularly in nano dimensions are particularly useful as bio-labels and for bio-imaging. The advantage of using near infrared radiation is that it is non-invasive and has high penetration depth. There is a very low probability of auto-fluorescence of the biological tissues if infrared radiation is used. It also involves a low cost near infrared continuous wave laser. Biological tissues only weakly absorb infrared radiation, thus preventing damage. Nano particles with Lanthanide ion embedded in inorganic matrix yield higher luminescence lifetimes, better quantum efficiencies and photo stability. Lanthanide doped materials are preferable as the emission mechanism is confined to the host lattice and remains unaffected by the outside environment. Such a situation is ideal for tagging in complicated bio systems. Hence, there is an increased emphasis on finding up-conversion materials, which can convert infrared wavelengths from 700 nm to 2000 nm into visible wavelengths.

The present work intends to find up-conversion phosphors that can be used in conversion of the infrared component in the solar radiation into visible radiation, so that it can be used in solar cells, particularly the Dye Sensitized Solar Cell.

Figure 4.1 shows the distribution of energy in the solar spectrum. It shows distinct peaks at 780 nm, 980 nm, 1250 nm and 1550 nm in the infrared region. While the visible component is 49% of the solar spectrum, the infrared component is 52%. As the solar cells absorb predominantly in the visible region to generate electricity, the conversion of infrared component into visible can increase the efficiency. The absorption range of different solar cells is given in figure 4.2.

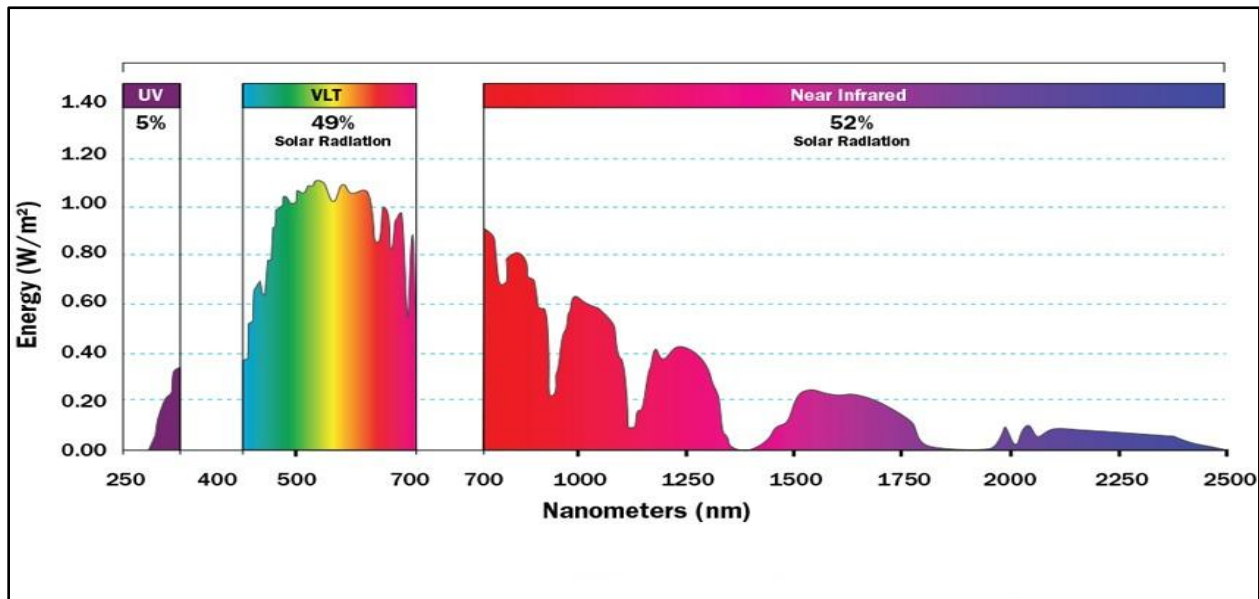


Figure 4.1: Distribution of energy in the solar spectrum {Courtesy: May-Mecho System [CE Centre – Advancing the Daylight]}

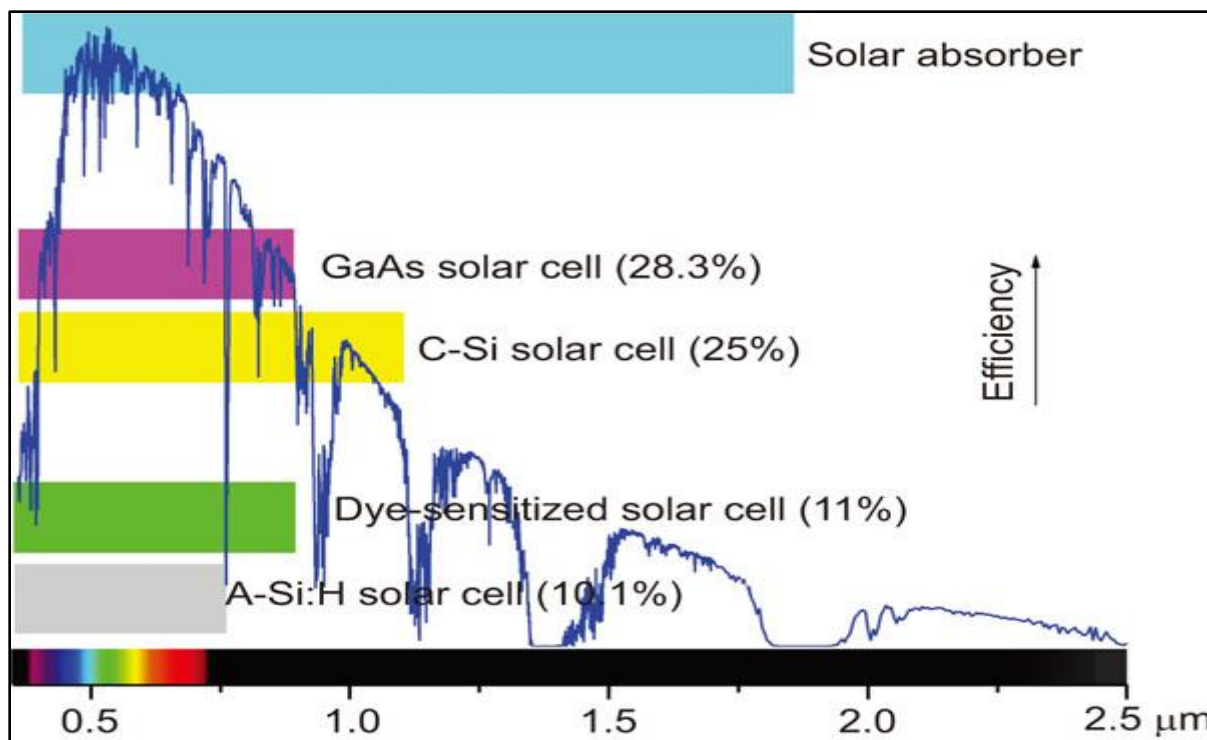


Figure 4.2: Absorption range in different Solar Cells {Courtesy: Light – Science and Applications (2014) 3 [doi:10.1038/lisa.2014.42]}

Attempts are being made to develop phosphors which absorb at different wavelengths in infrared region and convert them into visible light. Some of these materials, as mentioned above, include Erbium activated BaCl_2 with absorption at 800 nm, 970 nm and 1500 nm [17], Erbium activated Cerium Oxide absorbs at 785 nm [18]. $\text{Er}_2\text{Mo}_4\text{O}_{15}$ gives emission in visible region under 980 nm and 1550 nm excitation [19]. Erbium activated SrTiO_3 ultrafine powders with absorb at 785 nm [20]. Other materials which are excited by 980 nm laser diode are $\text{KMnF}_3:\text{Yb}^{3+}, \text{Er}^{3+}$ [21], $\text{NaYF}_4:\text{Yb}^{3+}, \text{Er}^{3+}$ [22], $\text{SrF}_2:\text{Yb}^{3+}, \text{Er}^{3+}$ [23], $\text{Y}_2\text{O}_3:\text{Yb}^{3+}, \text{Er}^{3+}$ [24], $\text{GdF}_3:\text{Yb}^{3+}, \text{Er}^{3+}$ [25], $\text{LiBaBO}_3:\text{Yb}^{3+}, \text{Er}^{3+}$ [26], $\text{LiNbO}_3:\text{Yb}^{3+}, \text{Er}^{3+}$ [27], $\text{Gd}_2\text{O}_3:\text{Yb}^{3+}, \text{Er}^{3+}$ [28], $\text{GdVO}_4:\text{Yb}^{3+}, \text{Er}^{3+}$ [29], $\text{ZnWO}_4:\text{Yb}^{3+}, \text{Er}^{3+}$ [30], $\text{LaF}_3:\text{Yb}^{3+}, \text{Er}^{3+}$ [31], $\text{ZrO}_2:\text{Yb}^{3+}, \text{Er}^{3+}$ [32], $\text{CaF}_2:\text{Yb}^{3+}, \text{Er}^{3+}$ [33].

4.6 Spectral characteristics of synthesized phosphors

The photoluminescence spectra of the synthesized samples were recorded using a fluorescence spectrometer with an excitation source of 980 nm. Similar amount of sample was taken for each of the recording. The results are given below.

4.6.1 $\text{La}_2(\text{MoO}_4)_3: \text{Yb}^{3+}, \text{Er}^{3+}$

Figures 4.3, 4.4 and 4.5 show the emission spectra of the three samples of $\text{La}_2(\text{MoO}_4)_3: \text{Yb}, \text{Er}$ with varying amount of Erbium in the increasing order, designated LMO 1, LMO 2 and LMO 3 respectively.

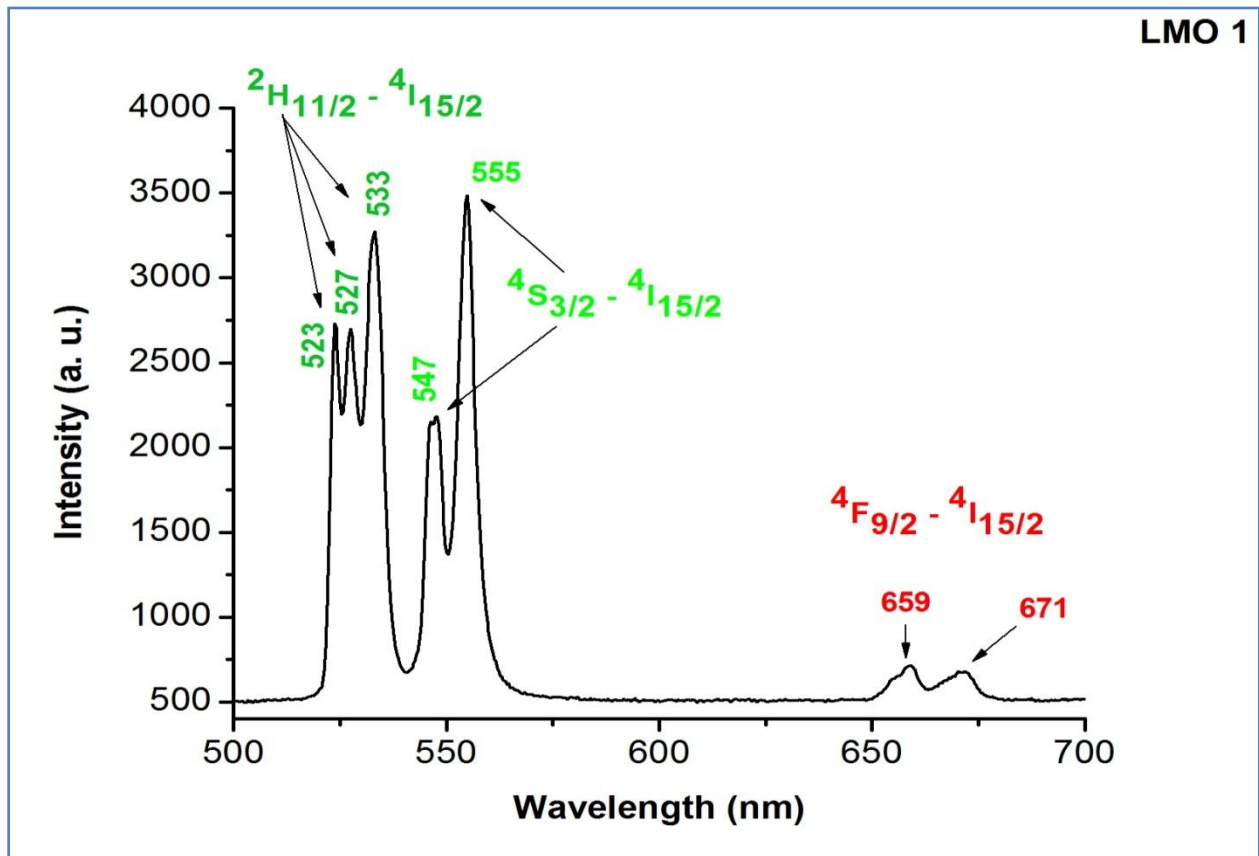


Figure 4.3: PL spectrum of sample LMO 1 $\{\text{La}_{2(0.79)}(\text{MoO}_4)_3: \text{Yb}_{(0.2)}, \text{Er}_{(0.01)}\}$

Sample LMO 1 as shown in Figure 4.3 gives strong emission at 523, 527 and 533 nm in the bluish green region as well as 547 and 555 nm in the green region. There are minor peaks at wavelengths 644, 659 and 671 nm in the red region. The peaks in the green region only contribute to the intensity as the intensity of peaks in the red region is insignificant.

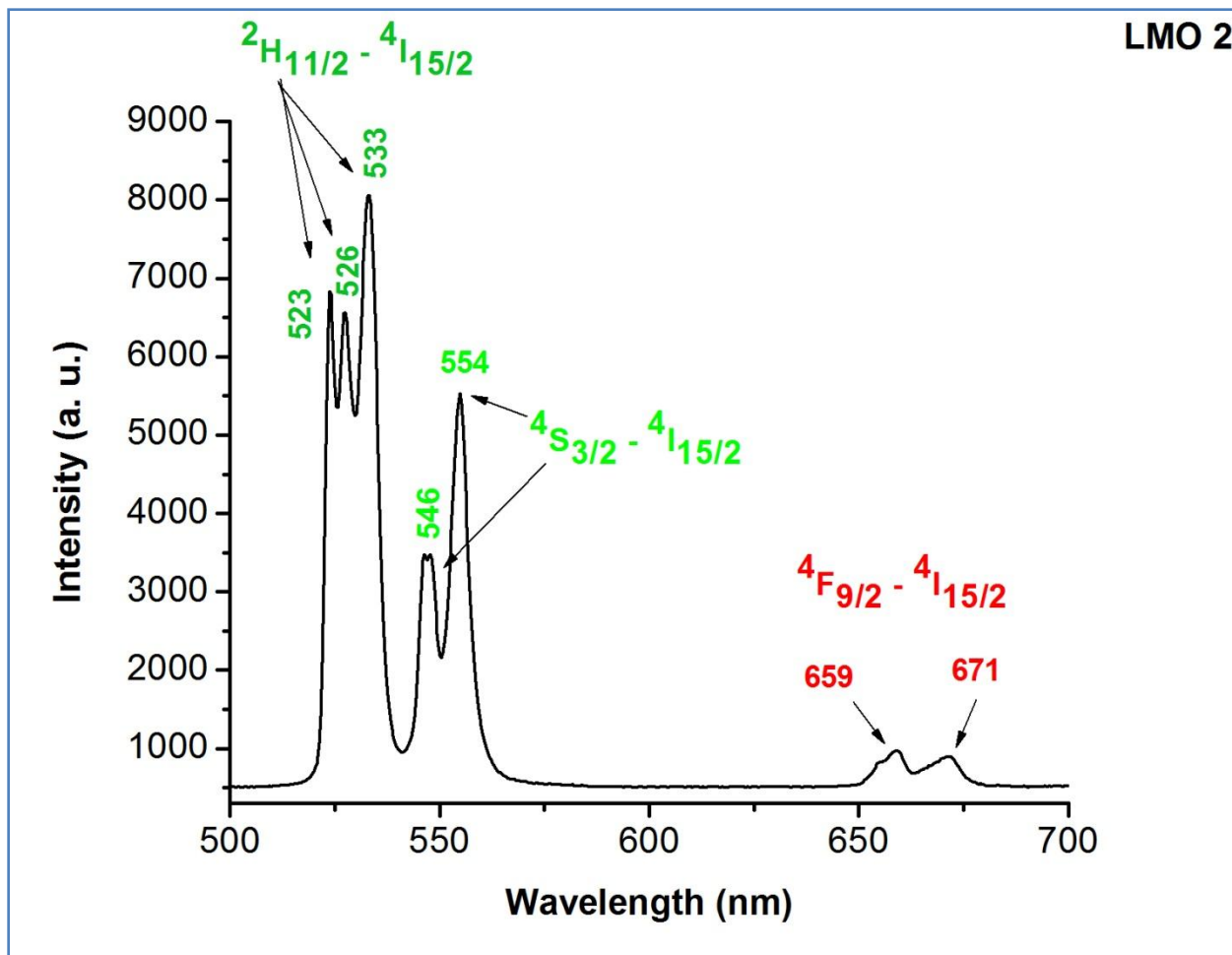


Figure 4.4: PL spectrum of sample LMO 2 $\{La_{2(0.78)}(MoO_4)_3: Yb_{(0.2)}, Er_{(0.02)}\}$

Sample LMO 2 gives similar emission at wavelengths of 523, 526, 533, 546, 554 nm in the bluish green as well as green region and at 659 and 671 nm in the red region as shown in Figure 4.4. Here too, the intensity of the green color emission is much higher.

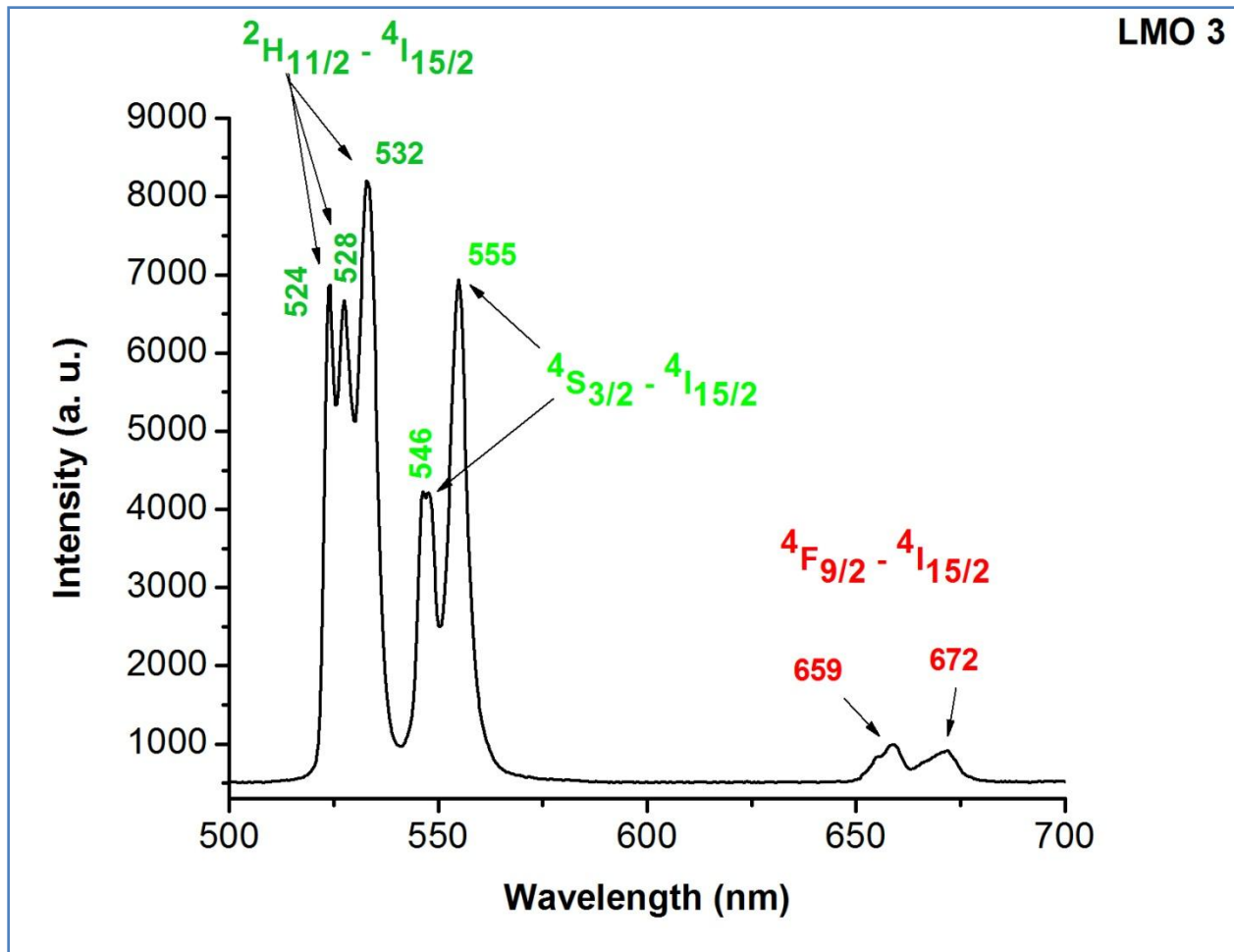


Figure 4.5: PL spectrum of sample LMO 3 $\{La_{2(0.77)}(MoO_4)_3: Yb_{(0.2)}, Er_{(0.03)}\}$

Figure 4.5 for the sample LMO 3 again shows emission peaks at wavelengths 524, 528, 532, 546 and 555 nm for bluish green and green color emission and at wavelengths 659 and 672 nm for red color emission. Here also, the intensity of the green color emission is high and of red color, emission is low.

The peaks in the bluish green region are attributed to the transition $2H_{11/2} \rightarrow 4I_{15/2}$ of Er^{3+} ion, while those in the green region are attributed to the transition $4S_{3/2} \rightarrow 4I_{15/2}$ of the same ion. Peaks in the red region are of $4F_{9/2} \rightarrow 4I_{15/2}$ transition of Er^{3+} . The free Er^{3+} ion would have an electron configuration $4f^{11}$. The lower term corresponding to this configuration is $4I_{15/2}$. However, in the

presence of crystal field, this level degenerates due to stark splitting giving multiple peaks for the transitions mentioned above [34]. This explains the multiplicity of peaks for each transition.

The changes in intensity of the peaks in all the three samples show a general trend as shown in Figure 4.6. It shows that there is increase in intensity of the peaks with increase in the amount of Erbium. The Erbium content increases from LMO 1 to LMO 3. At lower concentration of Erbium (sample LMO 1), the transition $^4S_{3/2} \rightarrow ^4I_{15/2}$ dominates as the intensity of the 555 nm peak is higher than the 533 nm peak of transition $^2H_{11/2} \rightarrow ^4I_{15/2}$. However, at higher concentrations of Erbium (samples LMO 2 and LMO 3), the transition $^2H_{11/2} \rightarrow ^4I_{15/2}$ corresponding to 533 nm clearly dominates over the other. Intensities due to the $^4F_{9/2} \rightarrow ^4I_{15/2}$ transition in the red region do not show any significant change.

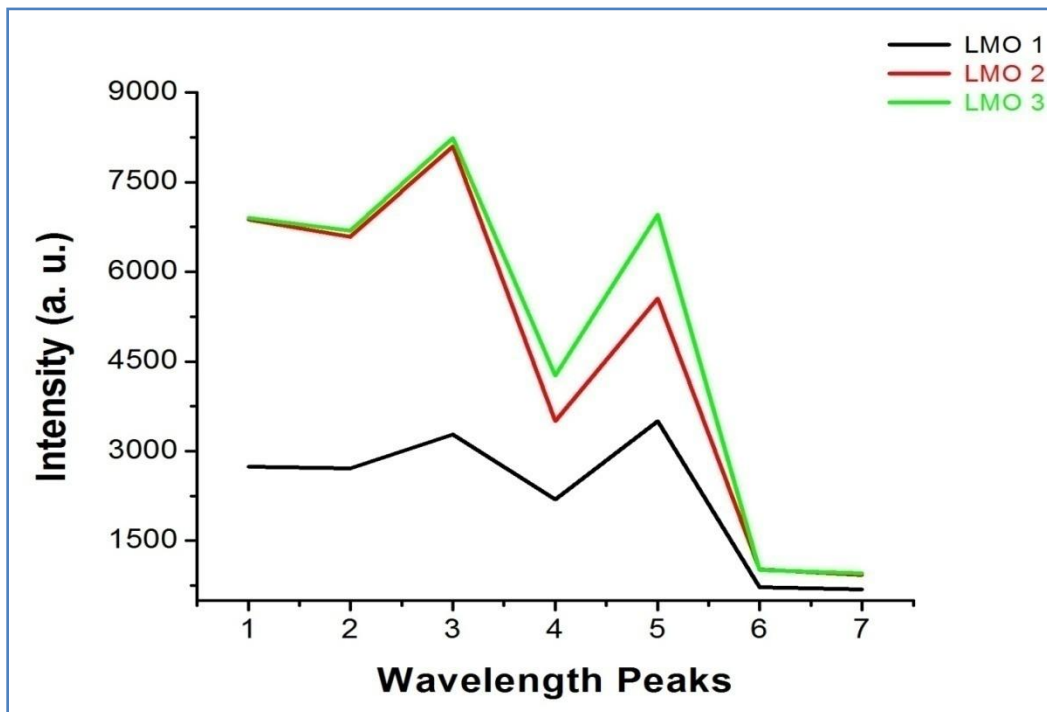


Figure 4.6: Changes in peak intensity in LMO samples

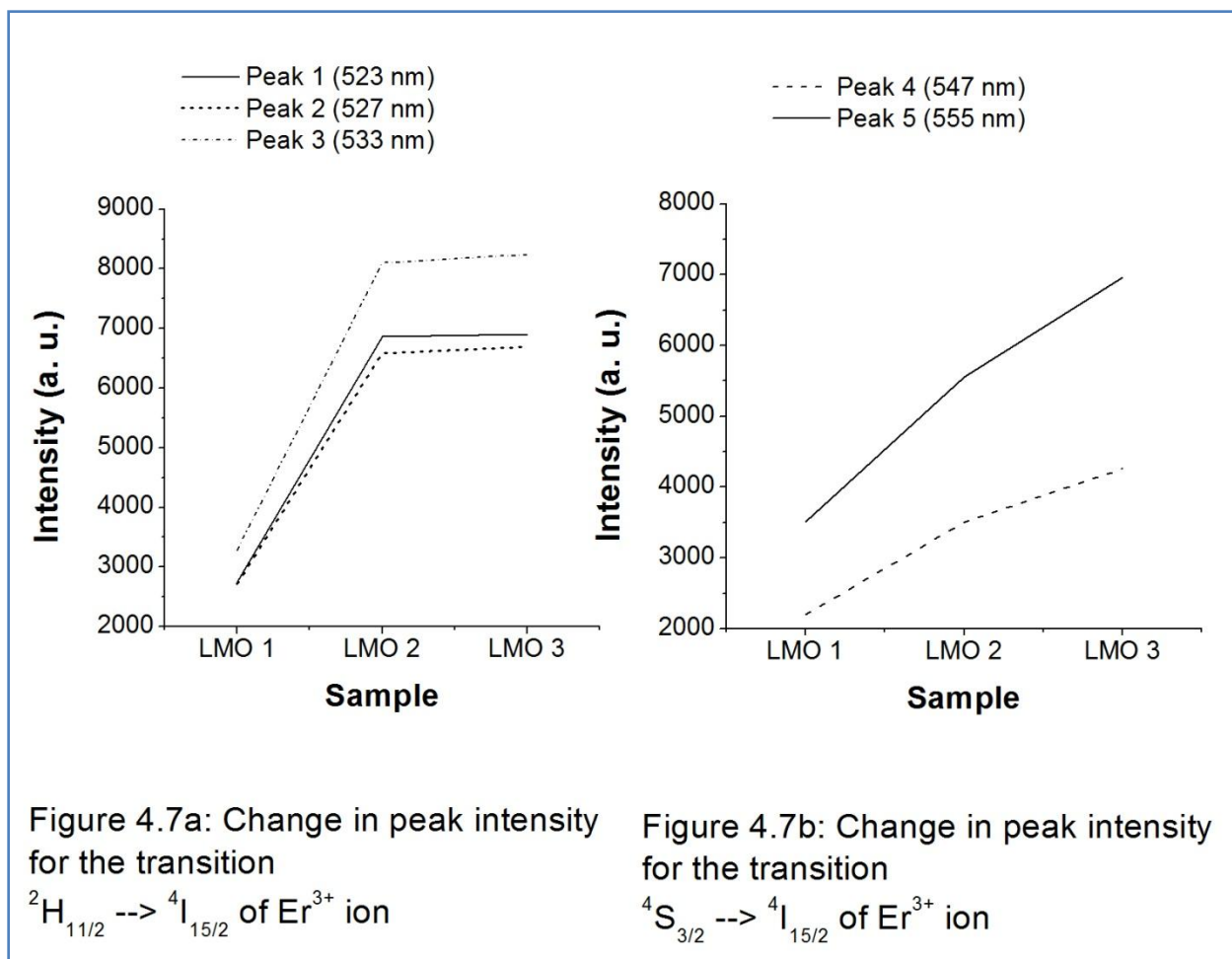


Figure 4.7a and 4.7b shows that the intensities of the peaks attributed to the transition ${}^2H_{11/2} \rightarrow {}^4I_{15/2}$ get saturated on increase in the Erbium content, while the intensities of the peaks attributed to the transition ${}^4S_{3/2} \rightarrow {}^4I_{15/2}$ increase almost linearly. In general, it is seen that by increasing the concentration of Erbium, there is an increase in the intensity of the emission peaks for green color emission.

The colour emitted by a phosphor can be visualized and understood by its position in the chromaticity diagram. For obtaining this position in terms of chromaticity coordinates, the emission characteristics of the samples were superimposed with the colour matching functions as shown in Figures 4.8 a, 4.8 b and 4.8 c. Colour matching functions are the amounts of primary

colours needed to match a particular colour. These primary colours have been standardized by CIE in 1931 as the RGB colour matching functions $r(\lambda)$, $g(\lambda)$ and $b(\lambda)$ corresponding to 700 nm, 546.1 nm and 435.8 nm respectively in the red, green and blue regions of the spectrum. The overlap between the emission spectra and the respective colour matching functions give the chromaticity coordinates of the emitted colour.

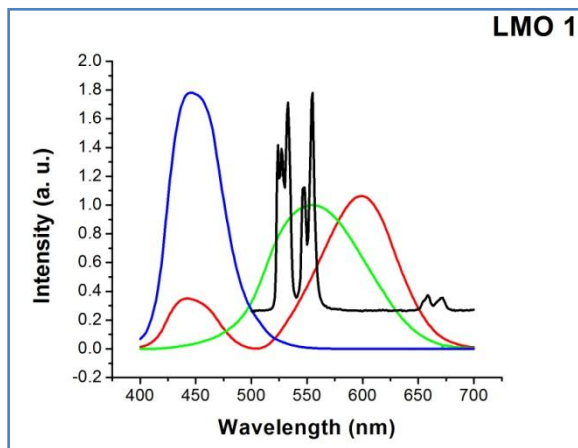


Figure 4.8 a

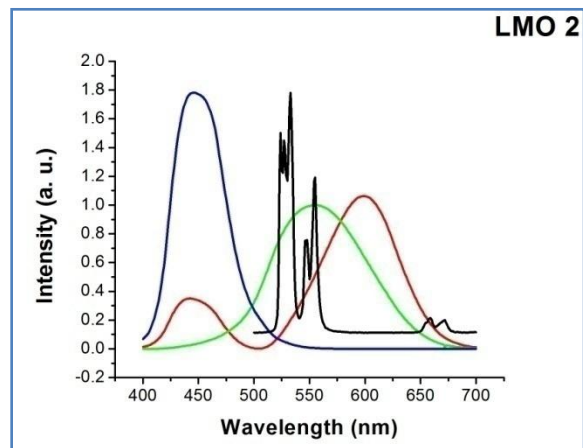


Figure 4.8 b

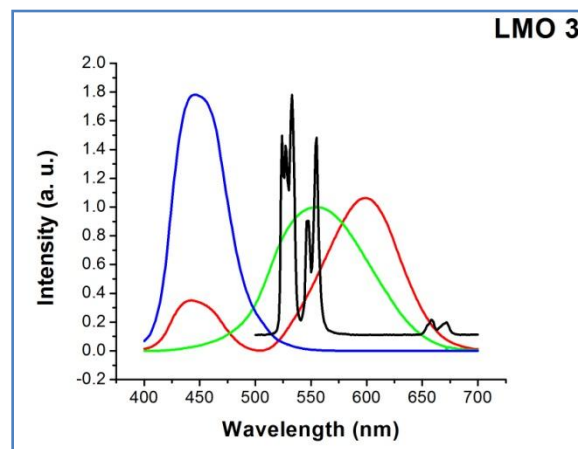


Figure 4.8 c

Overlapping of the emission spectra of samples with the colour matching functions.

The values of chromaticity coordinates calculated from the above diagram were plotted in the chromaticity diagram. Since the emission characteristics are different for the three samples, all the points are shown in the diagram inside the oval. The photograph of the emitted colour and the corresponding chromaticity diagram is given in Figure 4.9.

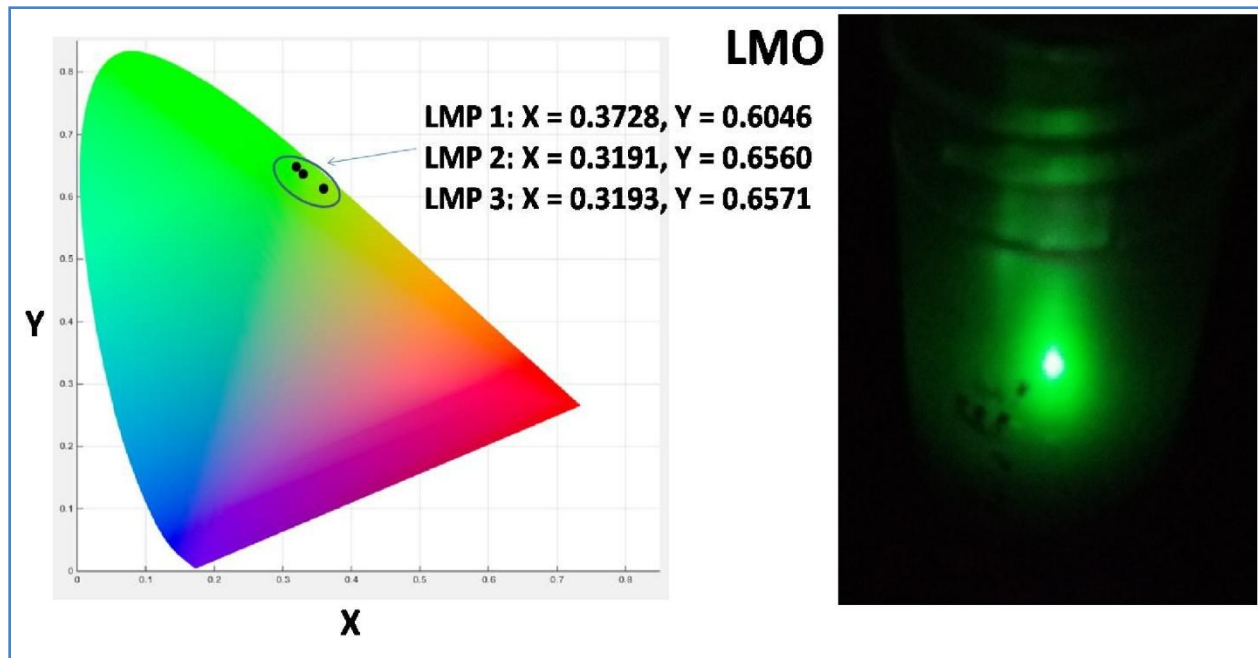


Figure 4.9: Photograph of the emitted colour and the corresponding chromaticity diagram

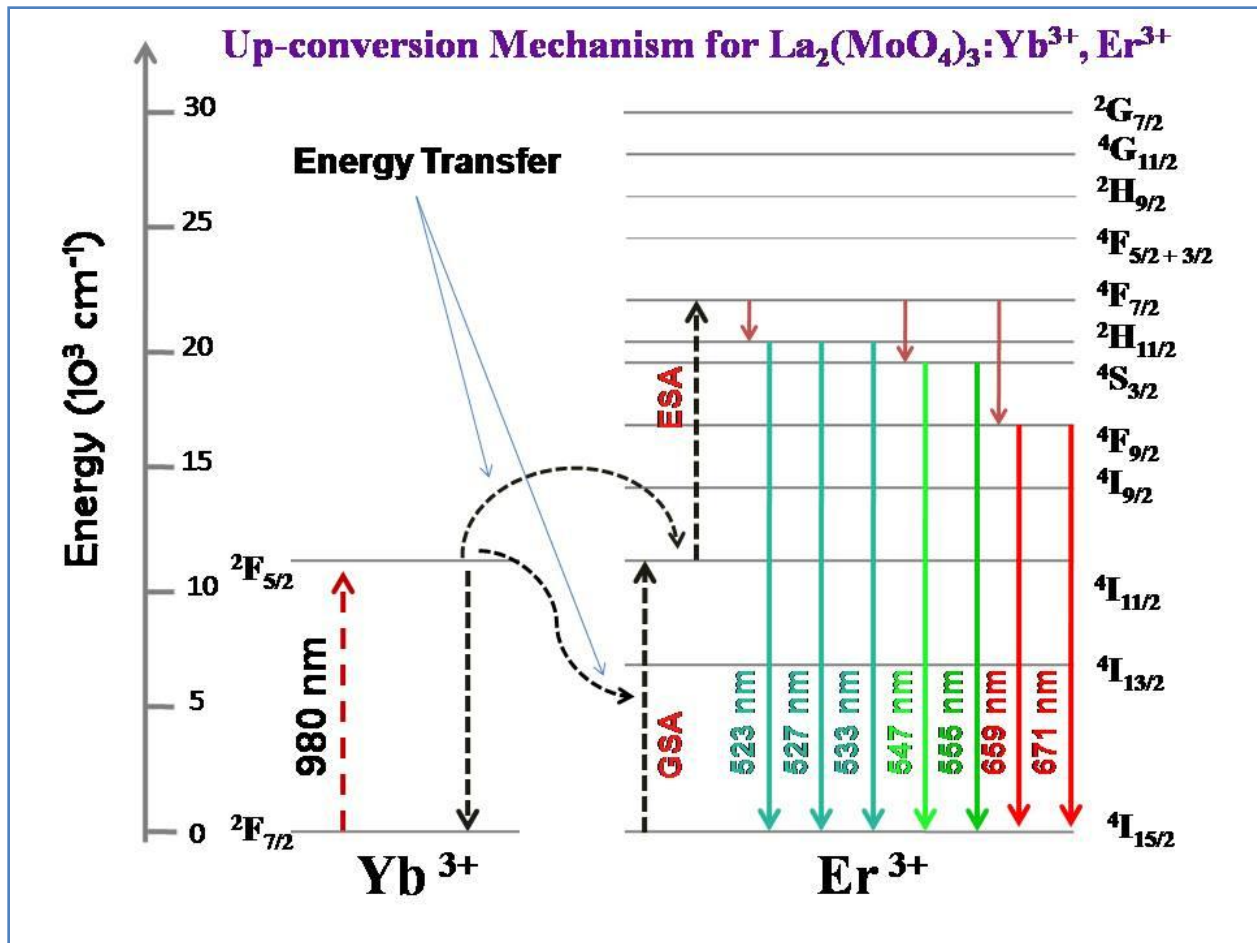


Figure 4.10: Mechanism of up conversion in $\text{La}_2(\text{MoO}_4)_3: \text{Yb}^{3+}, \text{Er}^{3+}$

Based on the emission characteristics, the up-conversion mechanism in $\text{La}_2(\text{MoO}_4)_3: \text{Yb}, \text{Er}$ can be described in the following steps, which is shown diagrammatically in Figure 4.10.

1. The 980 nm radiation is absorbed by the Yb^{3+} ions, as they have a much higher absorption cross section. It results in excitation of the Yb^{3+} ions from ${}^2\text{F}_{7/2} \rightarrow {}^2\text{F}_{5/2}$.
2. The de-excitation of Yb^{3+} ion from ${}^2\text{F}_{5/2} \rightarrow {}^2\text{F}_{7/2}$ leads to generation of photons with energy equal to the difference in energy levels, ${}^4\text{I}_{11/2}$ & ${}^4\text{I}_{15/2}$ as well as ${}^4\text{F}_{7/2}$ & ${}^4\text{I}_{11/2}$ of Er^{3+} ions.

3. In the next step, there is **Energy Transfer (ET)** of the energy generated as mentioned above, from Yb^{3+} ions (the sensitizer), to the Er^{3+} ions (the activator) in two different ways.

a) Energy transferred to Er^{3+} ions resulting in **Ground State Absorption (GSA)** in the Er^{3+} ion, which leads to excitation of these ions from ${}^4\text{I}_{15/2} \rightarrow {}^4\text{I}_{11/2}$.

b) Energy transferred to Er^{3+} ions resulting in **Excited State Absorption (ESA)** in the Er^{3+} ion, which leads to excitation of these ions from ${}^4\text{I}_{11/2} \rightarrow {}^4\text{F}_{7/2}$.

4. The electrons get accumulated at the ${}^4\text{F}_{7/2}$ level of Er^{3+} ion. Some of the electrons accumulated at the ${}^4\text{F}_{7/2}$ level release some energy non radiatively and reach ${}^2\text{H}_{11/2}$ level, from where their transition to the ${}^4\text{I}_{15/2}$ level results into the bluish green emission of the three peaks (523, 527 and 533 nm). $\{ {}^2\text{H}_{11/2} \rightarrow {}^4\text{I}_{15/2} \}$

Other electrons release more energy by non radiative transitions to reach ${}^4\text{S}_{3/2}$ level. Their transition to the ${}^4\text{I}_{15/2}$ level results into the emission of the two peaks (547 and 555 nm).

$\{ {}^4\text{S}_{3/2} \rightarrow {}^4\text{I}_{15/2} \}$

Few of these electrons release further energy at the ${}^4\text{S}_{3/2}$ level by non radiative means to reach the ${}^4\text{F}_{9/2}$ level. These electrons transit to the ${}^4\text{I}_{15/2}$ level to give emission in the red region. $\{ {}^4\text{F}_{9/2} \rightarrow {}^4\text{I}_{15/2} \}$

4.6.2 $\text{Bi}_2\text{O}_3: \text{Yb}^{3+}, \text{Er}^{3+}$

Photoluminescence spectra of the samples BO 1, BO 2 and BO 3 were taken using NIR excitation at 980 nm wavelength. Figures 4.11, 4.12 and 4.13 show the emission spectra of samples BO 1, BO 2 and BO 3 respectively. All the samples show a single emission peak at 510 nm, which can be attributed to the transition ${}^2\text{H}_{11/2} \rightarrow {}^4\text{I}_{15/2}$. The peaks are very narrow with a value of full width at half maximum below 1 nm.

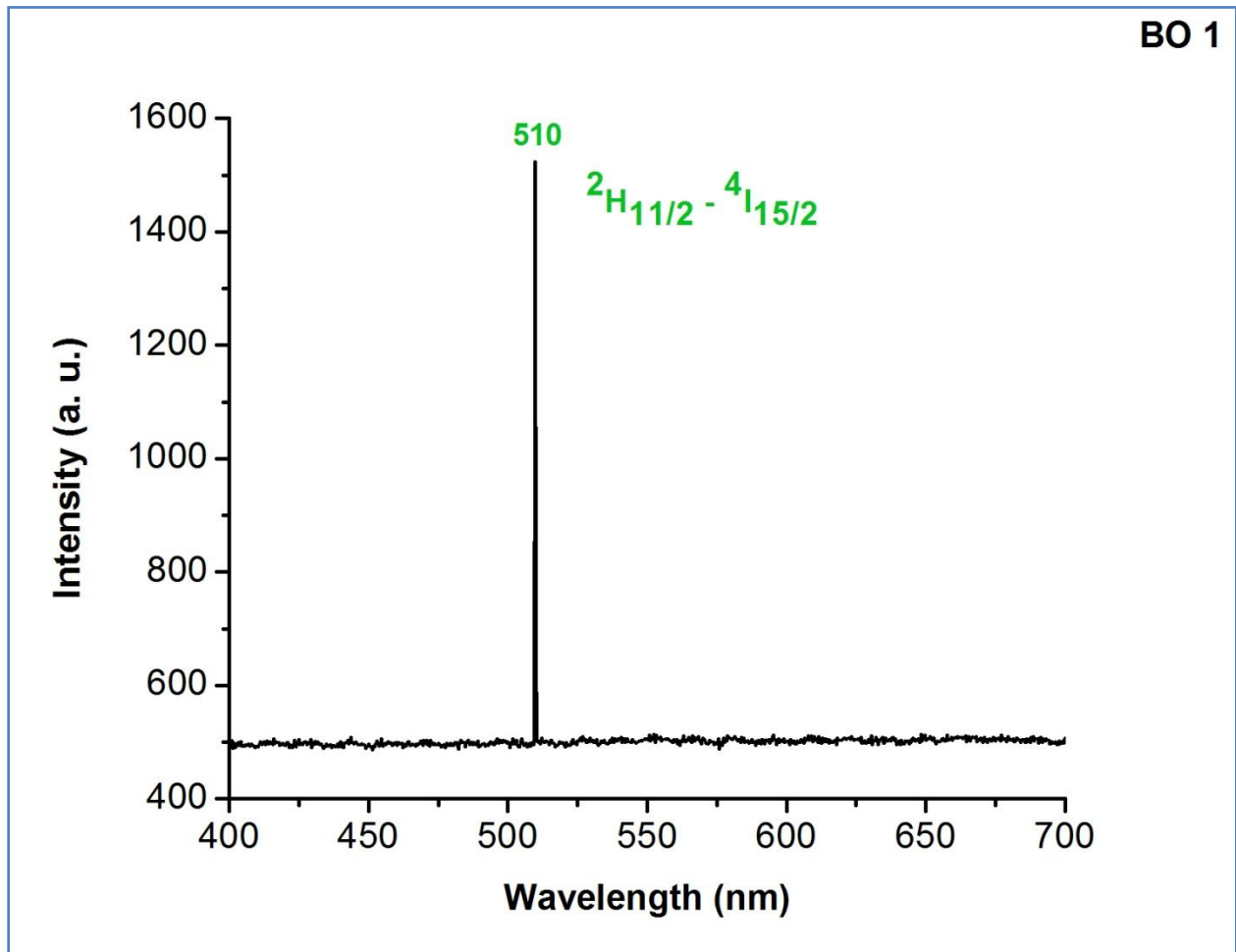


Figure 4.11: PL spectrum of sample BO 1 $\{\text{Bi}_2\text{O}_3: \text{Yb}_{(0.2)}, \text{Er}_{(0.01)}\}$

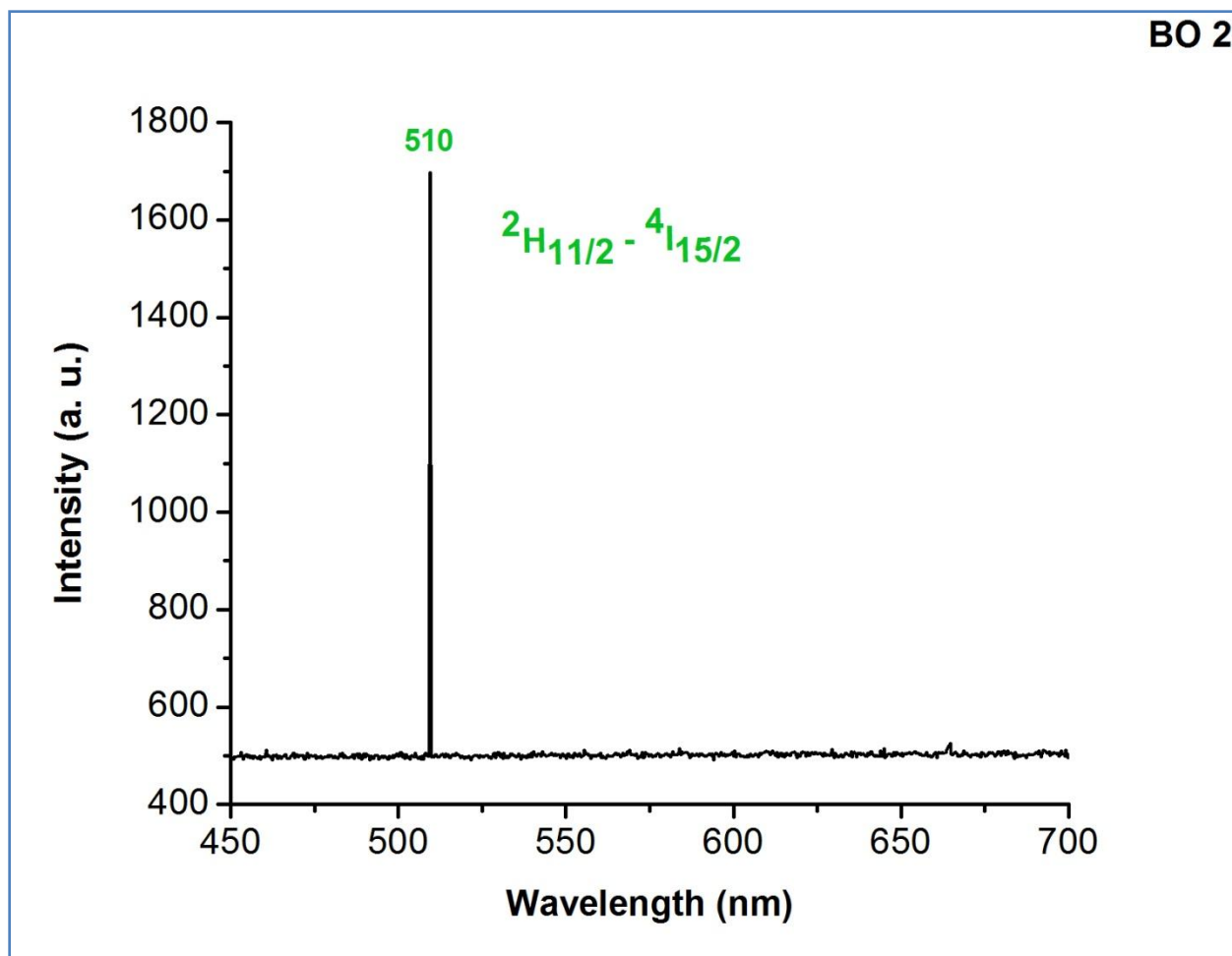


Figure 4.12: PL spectrum of sample BO 2 $\{Bi_2O_3: Yb_{(0.2)}, Er_{(0.02)}\}$

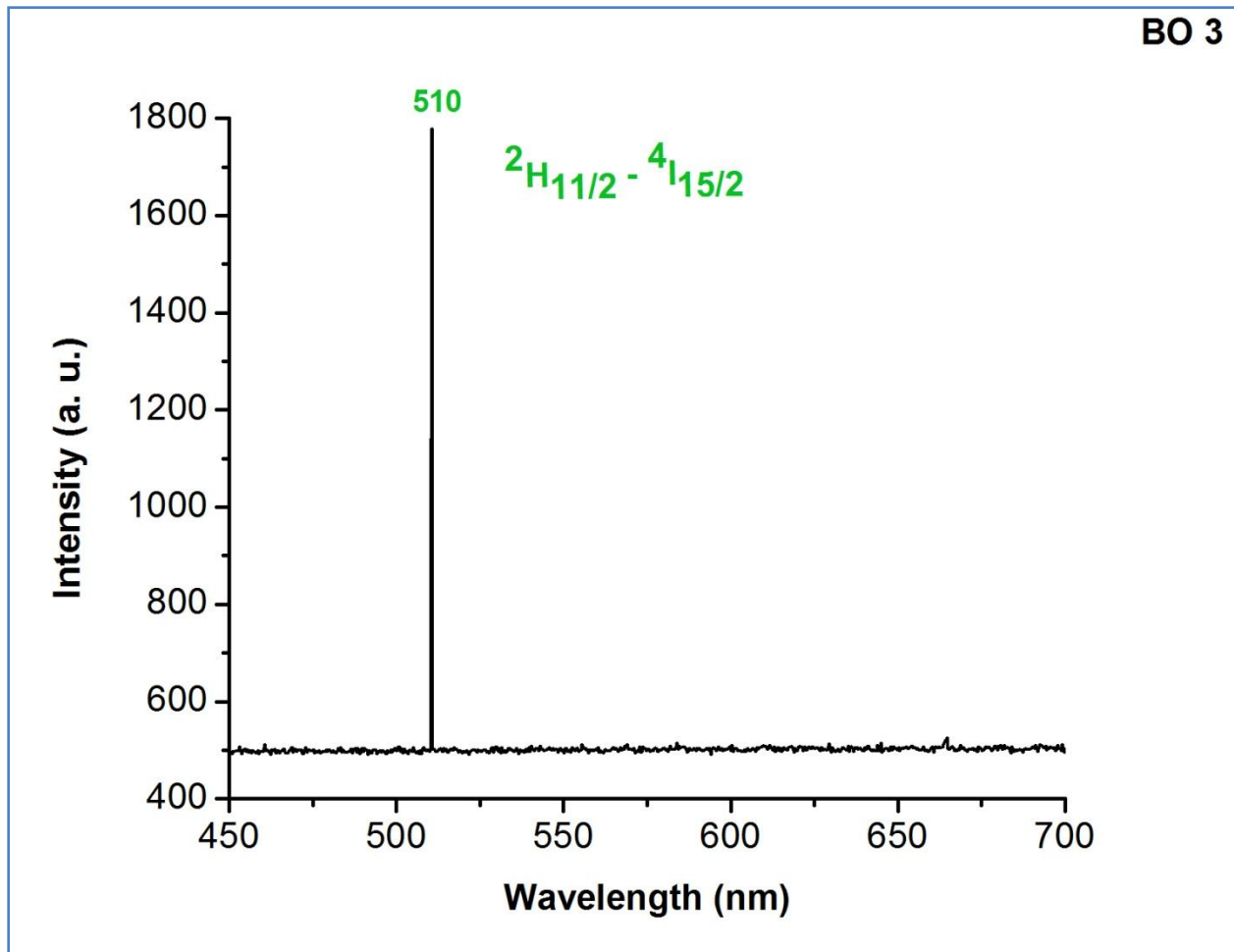


Figure 4.13: PL spectrum of sample BO 3 $\{Bi_2O_3: Yb_{(0.2)}, Er_{(0.03)}\}$

It can be seen from the figure 4.14 given below that the intensity of the samples increase with the Erbium content.

A similar exercise as mentioned earlier was carried out for the BO samples to find out the chromaticity coordinates. A spectrum of only one sample as given in figure 4.15 below was taken for the purpose as there is no change in the wavelengths of emission in the three samples. The photograph of the emitted colour and the corresponding chromaticity diagram is given in Figure 4.16.

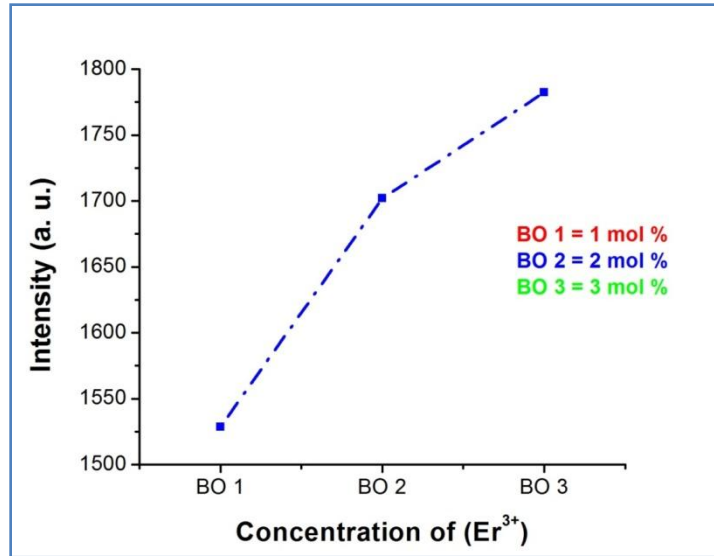


Figure 4.14: Change in intensity with Er content (for BO samples)

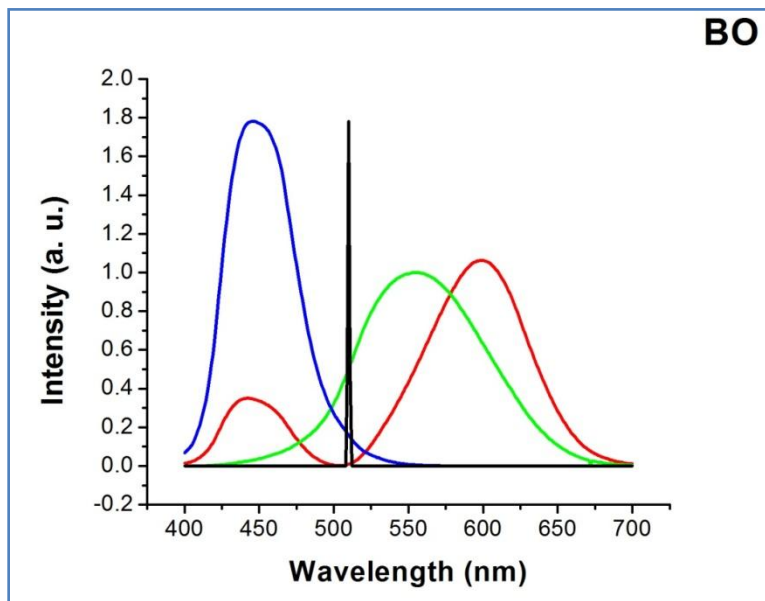


Figure 4.15: Overlapping of the emission spectrum of Bi₂O₃:Yb³⁺, Er³⁺ with the colour matching functions.

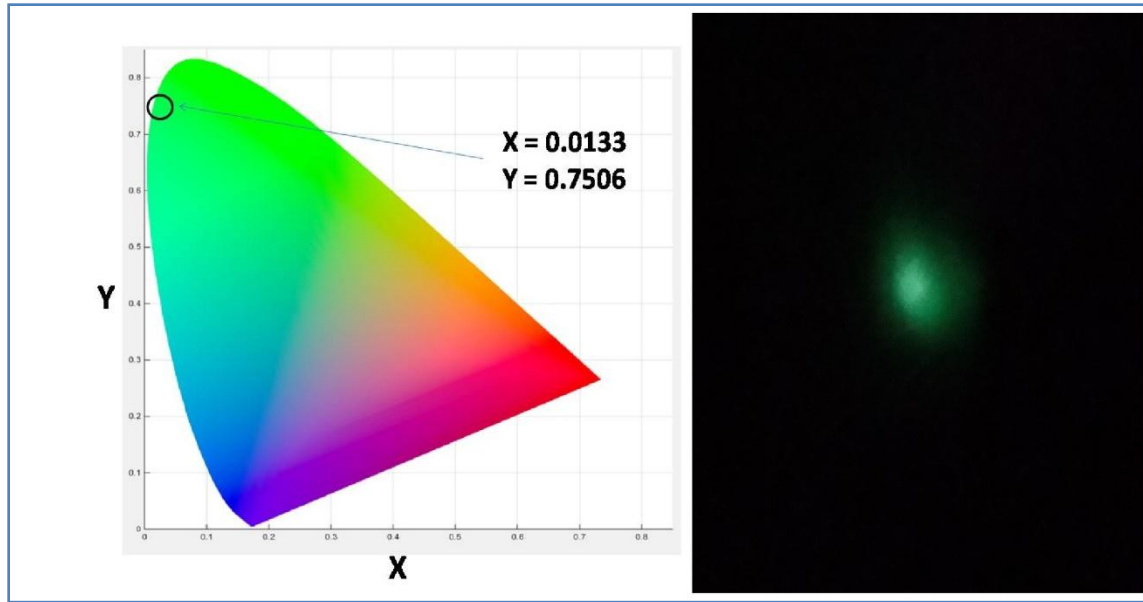


Figure 4.16: Photograph of the emitted colour and the corresponding chromaticity diagram

Based on the emission characteristics, the up-conversion mechanism in $\text{Bi}_2\text{O}_3: \text{Yb}, \text{Er}$ can be described in the following steps, which is shown diagrammatically in Figure 4.17.

1. The 980 nm radiation is absorbed by the Yb^{3+} ion, resulting in the excitation of the Yb^{3+} ion from $^2\text{F}_{7/2} \rightarrow ^2\text{F}_{5/2}$.
2. The de-excitation of Yb^{3+} ion from $^2\text{F}_{5/2} \rightarrow ^2\text{F}_{7/2}$ leads to generation of photons.
3. In the next step, there is **Energy Transfer (ET)** of the energy generated as mentioned above, from Yb^{3+} ions (the sensitizer), to the Er^{3+} ions (the activator) in two different ways.
 - c) Energy transferred to Er^{3+} ions resulting in **Ground State Absorption (GSA)** in the Er^{3+} ion, which leads to excitation of these ions from $^4\text{I}_{15/2} \rightarrow ^4\text{I}_{11/2}$.
 - d) Energy transferred to Er^{3+} ions resulting in **Excited State Absorption (ESA)** in the Er^{3+} ion, which leads to excitation of these ions from $^4\text{I}_{11/2} \rightarrow ^4\text{F}_{7/2}$.

4. The electrons get accumulated at the $^4F_{7/2}$ level of Er^{3+} ion. The electrons accumulated at the $^4F_{7/2}$ level release energy non radiatively and reach $^2H_{11/2}$ level, from where their transition to the $^4I_{15/2}$ level results into the red emission of 510 nm. $\{ ^2H_{11/2} \rightarrow ^4I_{15/2} \}$

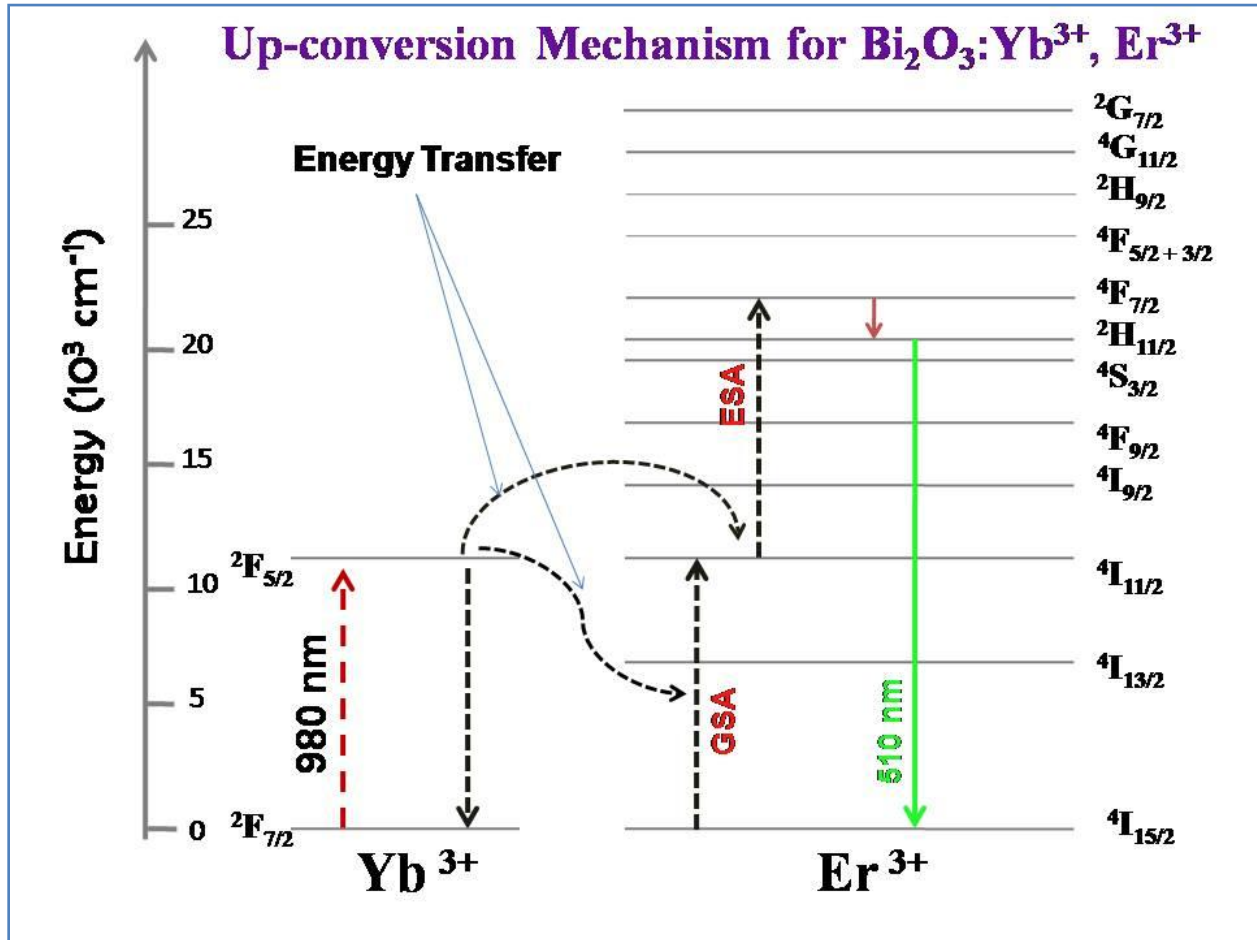


Figure 4.17: Mechanism of up conversion in $\text{Bi}_2\text{O}_3:\text{Yb}^{3+}, \text{Er}^{3+}$

4.6.3 CdO: Yb³⁺, Er³⁺

Photoluminescence spectra of all samples CO 1, CO 2 and CO 3 were taken using NIR excitation at 980 nm wavelength. Figures 4.18, 4.19 and 4.20 show the emission spectra of samples CO 1, CO 2 and CO 3 respectively.

Figure 4.18 for CO 1 shows one sharp and narrow emission peak at 626 nm in the red region. Figure 4.19 also shows the same feature at 627 nm for CO 2 sample with almost the same intensity as in case of CO 1 sample. Figure 4.20 for CO 3 sample shows a similar feature at 630 nm with much higher intensity.

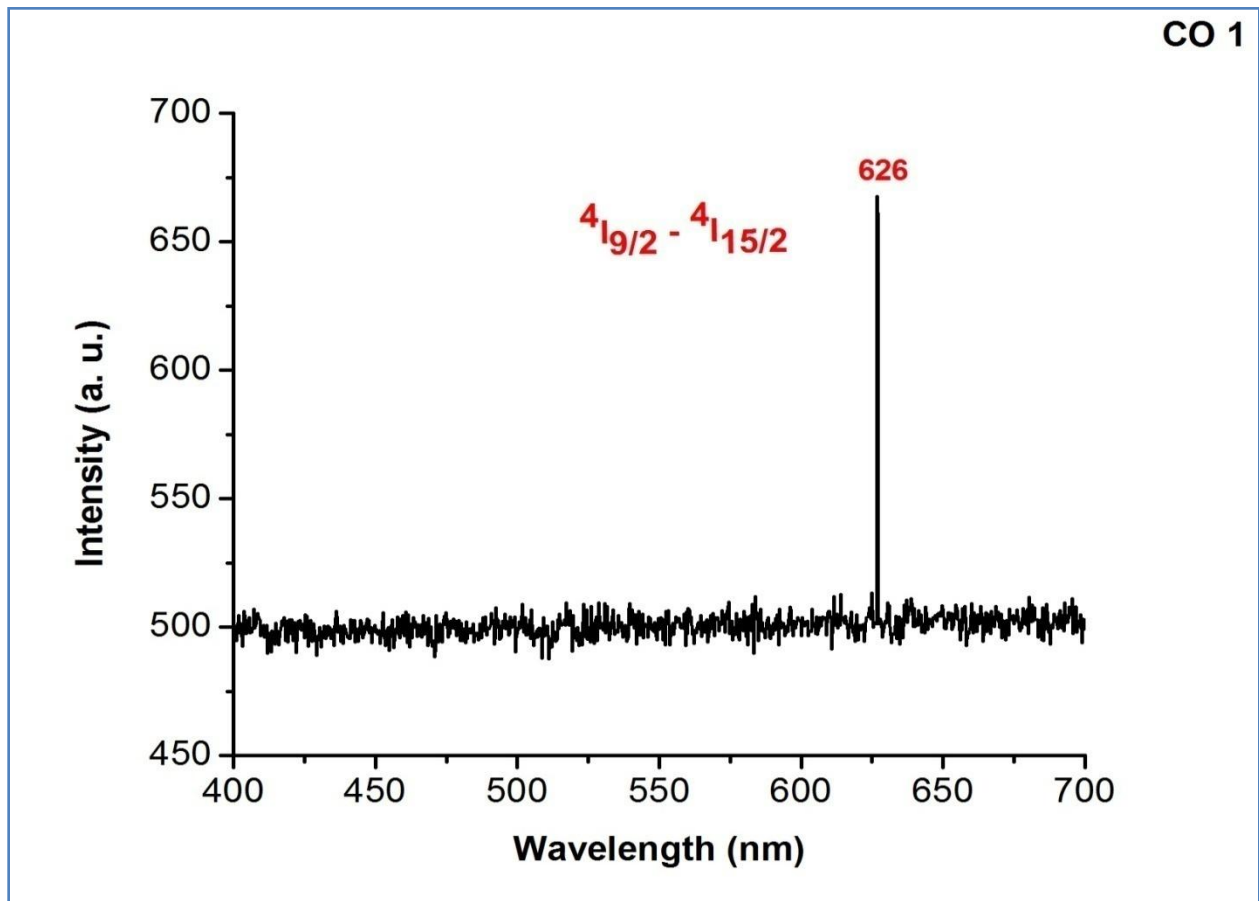


Figure 4.18: PL spectrum of sample CO 1 { CdO: Yb_(0.2), Er_(0.01) }

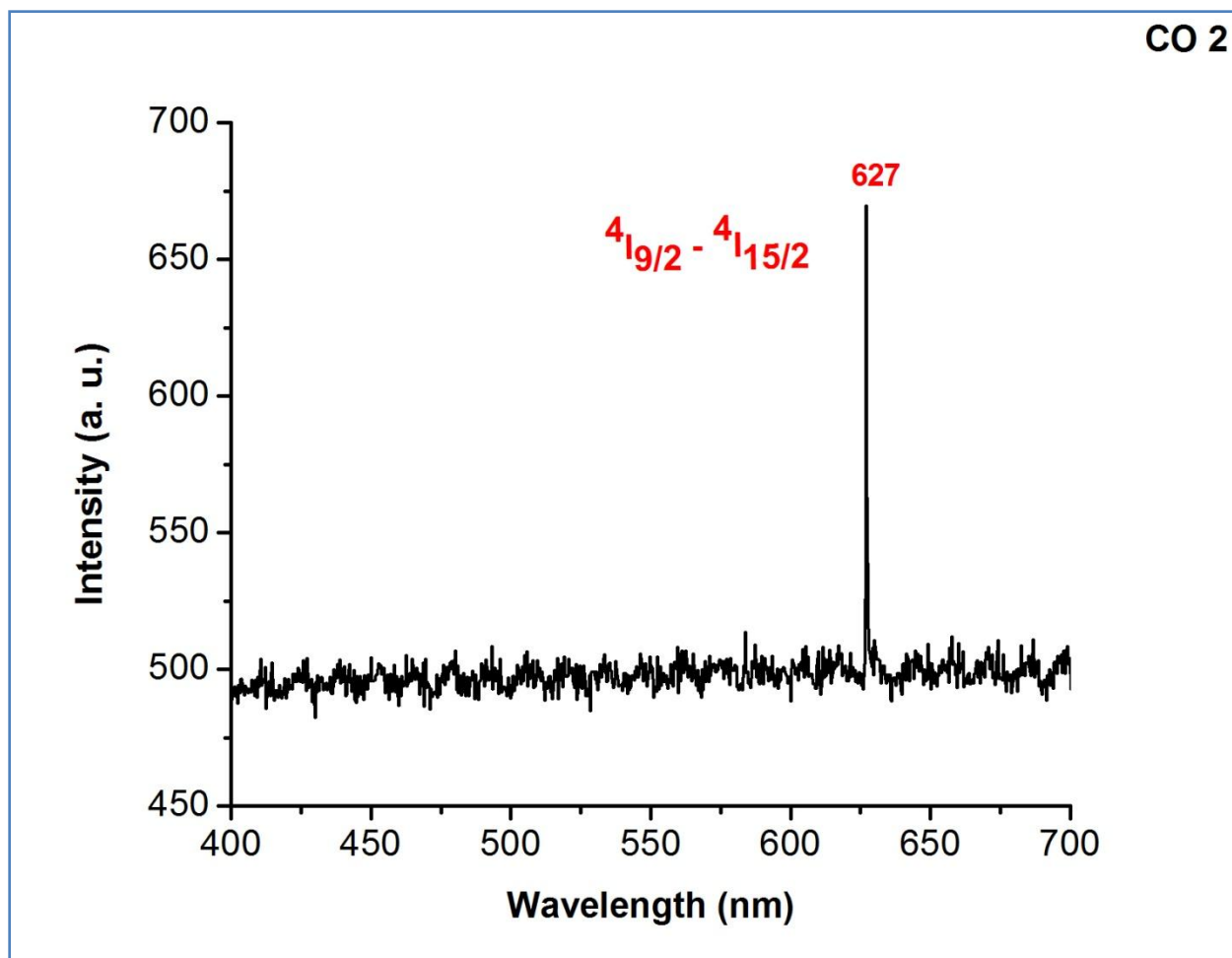


Figure 4.19: PL spectrum of sample CO 2 { $CdO: Yb_{(0.2)}, Er_{(0.02)}$ }

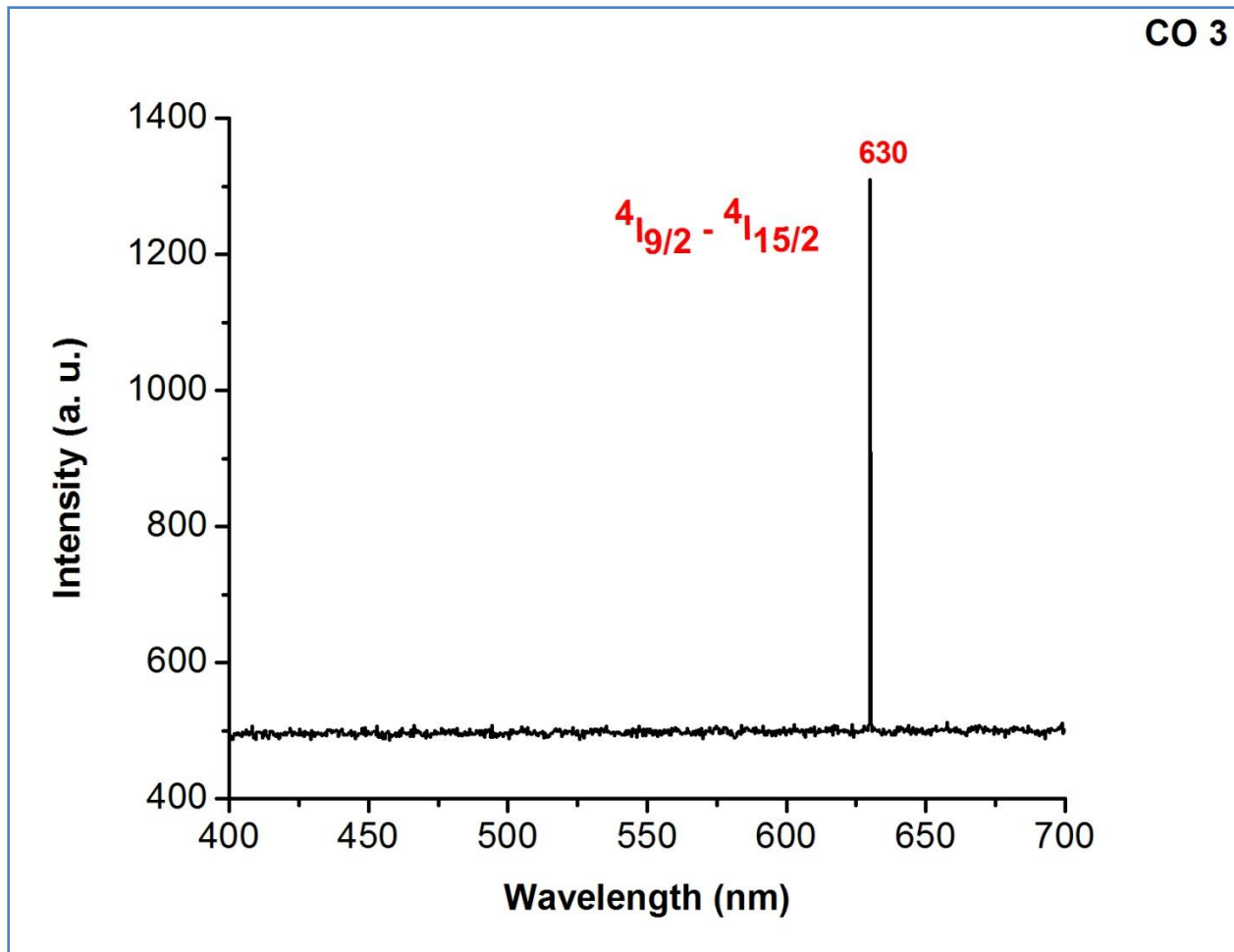


Figure 4.20: PL spectrum of sample CO 3 { $CdO: Yb_{(0.2)}, Er_{(0.03)}$ }

The full width at half maximum for the first two samples (CO 1 & CO 2) is around 0.5 nm, while it is still less for the third sample (CO 3). Hence the peaks are very narrow and sharp. This peak is attributed to the transition ${}^4I_{9/2} \rightarrow {}^4I_{15/2}$ of the Er^{3+} ion. The slight shift in the wavelength is due to the crystal field.

It can be seen from Figure 4.21 that the intensity of emission is the highest for the sample with maximum Erbium content. Since CdO has not been studied for up conversion so far, these results open the possibility of studying it further with still higher Erbium content.

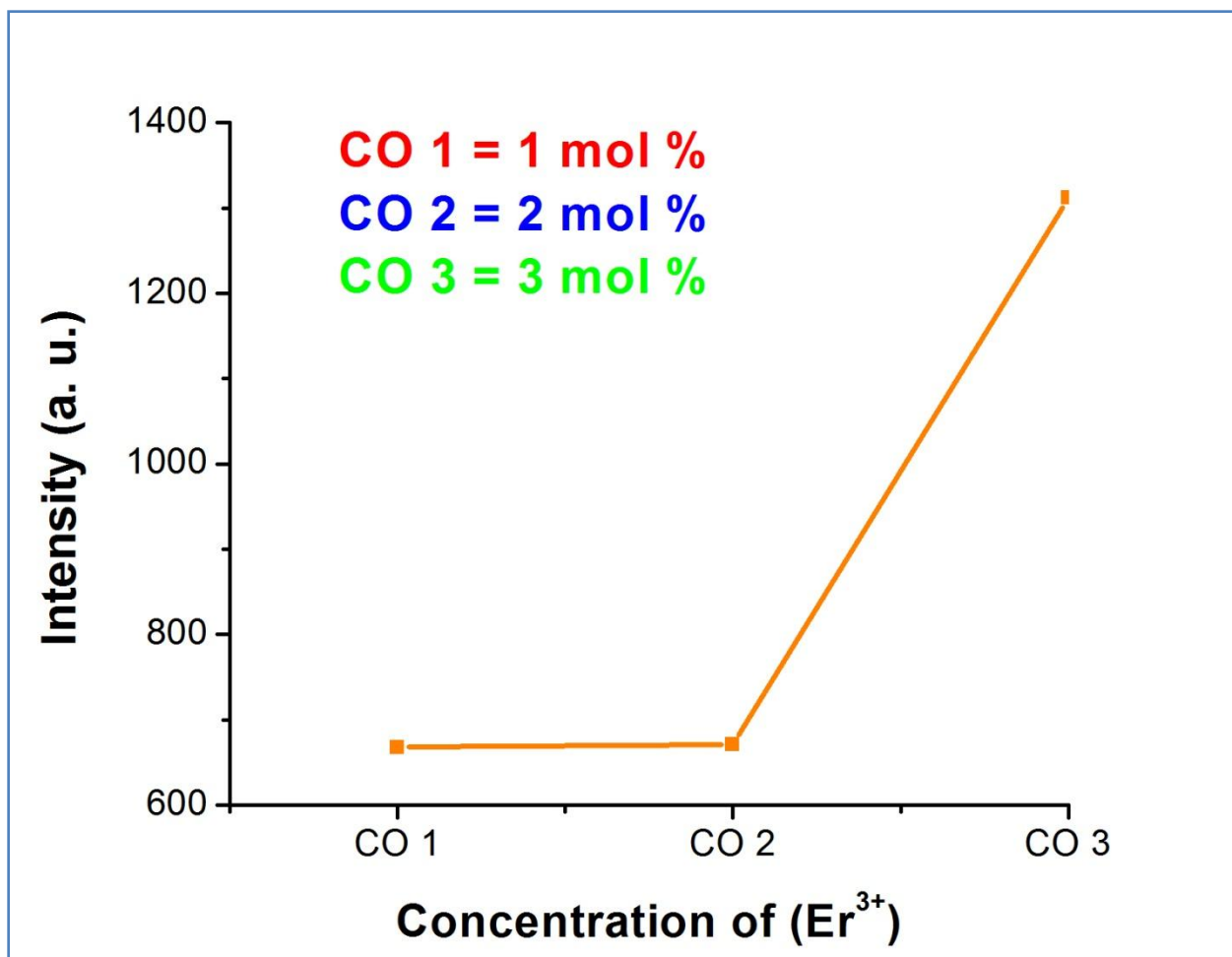


Figure 4.21: Change in intensity with Er³⁺ content (for CO samples)

A similar exercise as mentioned earlier for LMO samples was carried out for the CO samples to find out the chromaticity coordinates. A spectrum of only one sample as mentioned in figure 4.22, was taken for the purpose as there is no appreciable change in the wavelengths of emission in the three samples. The photograph of the emitted colour and the corresponding chromaticity diagram is given in Figure 4.23.

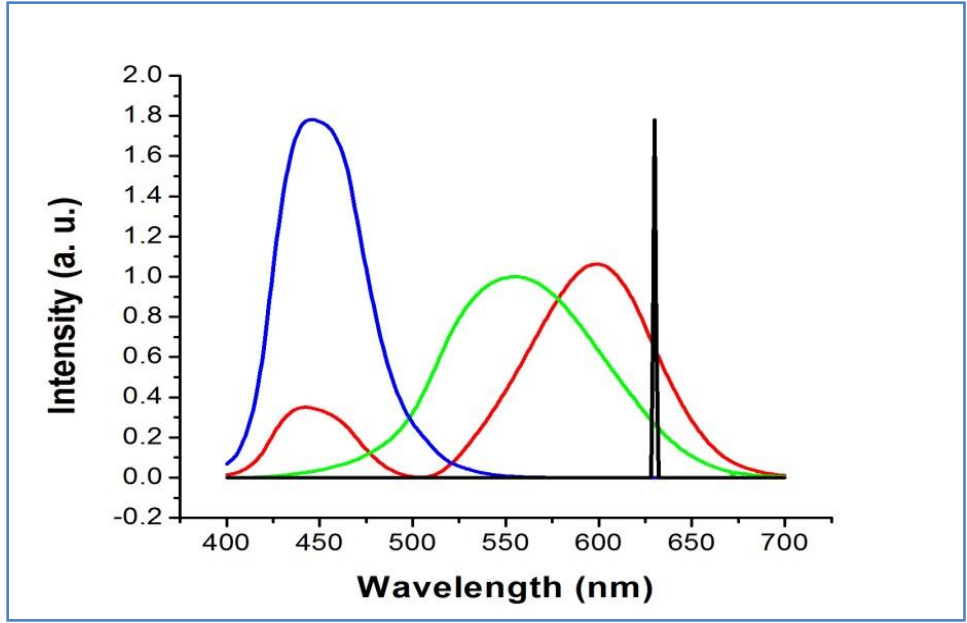


Figure 4.22: Overlapping of the emission spectrum of CdO: Yb³⁺, Er³⁺ with the colour matching functions.

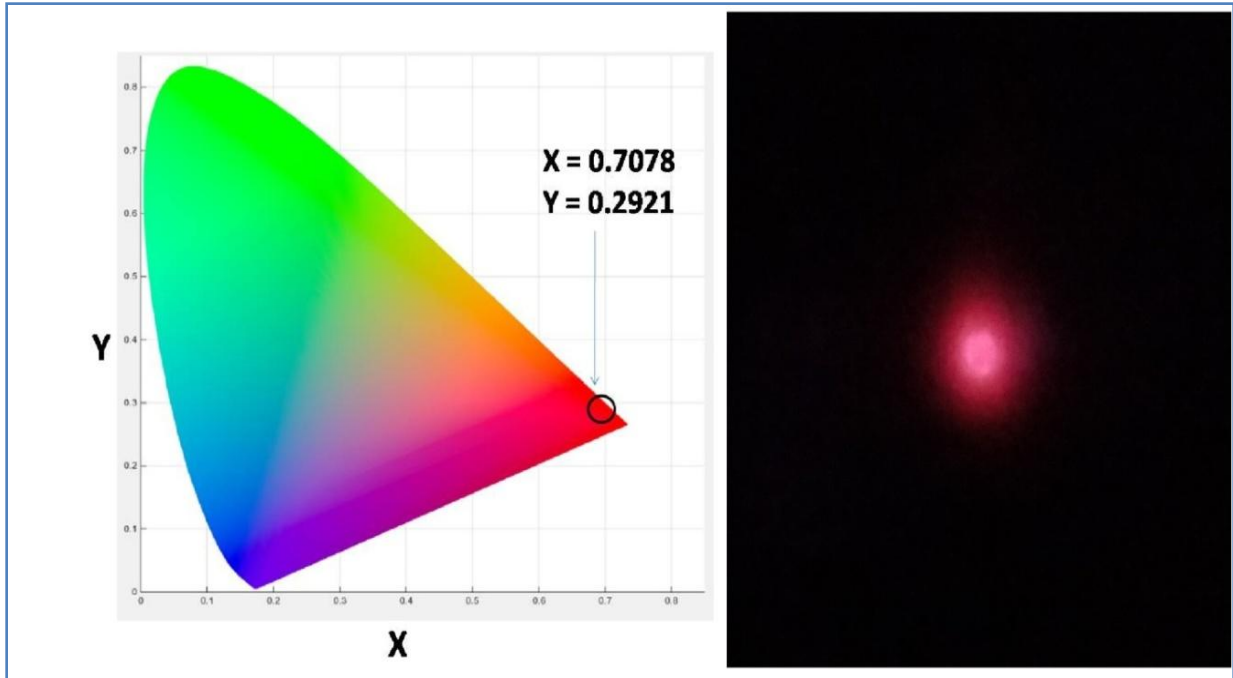


Figure 4.23: Photograph of the emitted colour and the corresponding chromaticity diagram

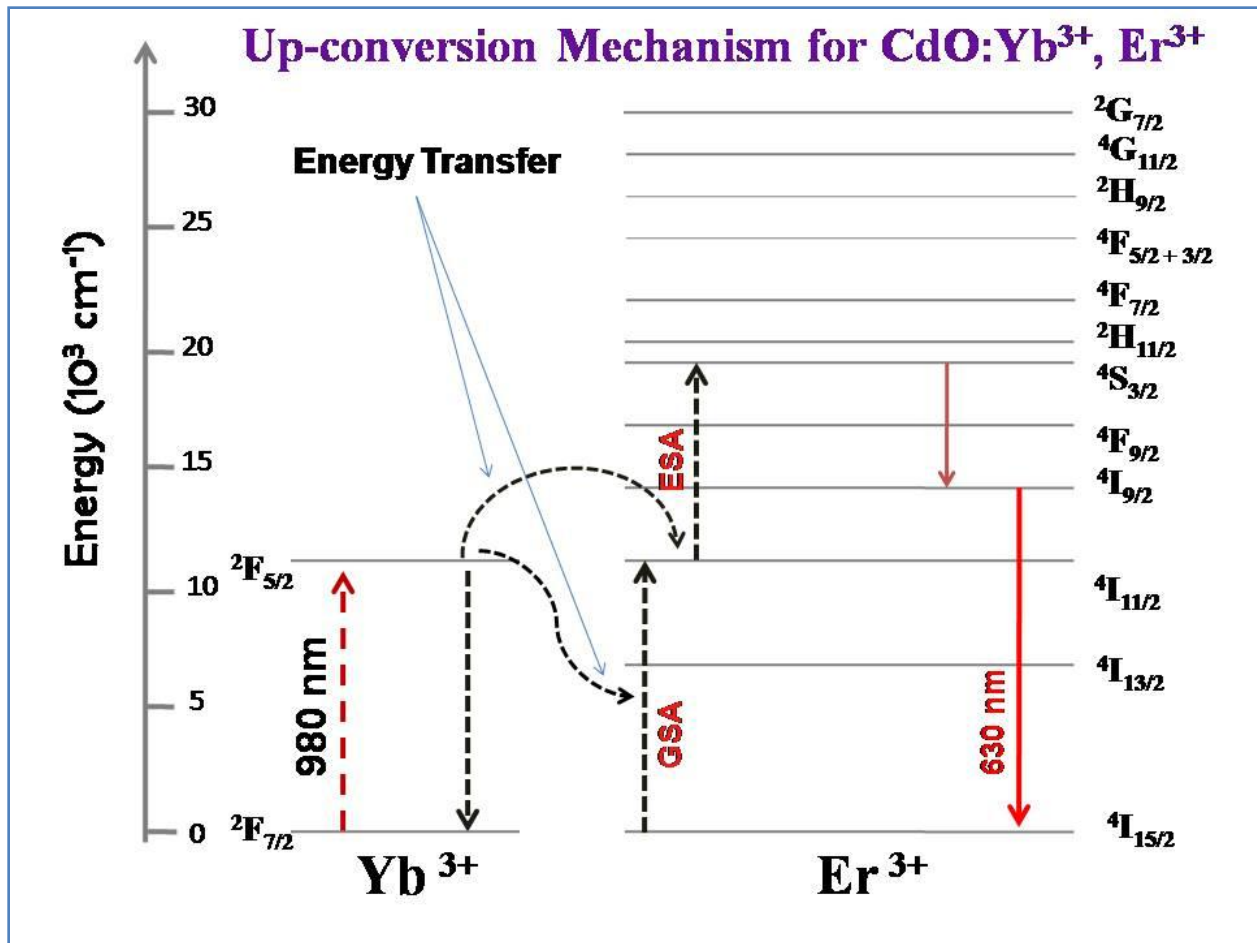


Figure 4.24: Mechanism of up conversion in CdO: Yb³⁺, Er³⁺

Based on the emission characteristics, the up-conversion mechanism in CdO: Yb, Er can be described in the following steps, which is shown diagrammatically in Figure 4.24.

1. The 980 nm radiation is absorbed by the Yb³⁺ ion, resulting in the excitation of the Yb³⁺ ion from $^2F_{7/2} \rightarrow ^2F_{5/2}$.
2. The de-excitation of Yb³⁺ ion from $^2F_{5/2} \rightarrow ^2F_{7/2}$ leads to generation of photons.
3. In the next step, there is **Energy Transfer (ET)** of the energy generated as mentioned above, from Yb³⁺ ions (the sensitizer), to the Er³⁺ ions (the activator) in two different ways.

4. Energy transferred to Er^{3+} ions resulting in **Ground State Absorption (GSA)** in the Er^{3+} ion, which leads to excitation of these ions from ${}^4\text{I}_{15/2} \rightarrow {}^4\text{I}_{11/2}$.
5. Energy transferred to Er^{3+} ions resulting in **Excited State Absorption (ESA)** in the Er^{3+} ion, which leads to excitation of these ions from ${}^4\text{I}_{11/2} \rightarrow {}^4\text{S}_{3/2}$.
6. The electrons get accumulated at the ${}^4\text{S}_{3/2}$ level of Er^{3+} ion. The electrons accumulated at the ${}^4\text{S}_{3/2}$ level release energy non radiatively and reach ${}^4\text{I}_{9/2}$ level, from where their transition to the ${}^4\text{I}_{15/2}$ level results into the red emission of 630 nm. $\{ {}^4\text{I}_{9/2} \rightarrow {}^4\text{I}_{15/2} \}$

4.7 Summary

The phosphor samples synthesized to study up-conversion characteristics were excited by 980 nm radiation.

All the samples give up-conversion luminescence. The samples of $\text{La}_2(\text{MoO}_4)_3$: Yb, Er give major emissions in the green and some emission in the red region. The emission with multiple peaks is attributed to the Er^{3+} ions, while Yb^{3+} acts as a sensitizer. There is splitting of peaks in the bluish green and green regions on account of the Stark effect due to the crystal field of the host material. An increase in intensity is observed in the green region with increase in the Erbium content.

In case of Bi_2O_3 : Yb, Er, all the samples exhibit a single narrow and intense peak at 510 nm. It is attributed to the ${}^2\text{H}_{11/2} \rightarrow {}^4\text{I}_{15/2}$ transition of Er^{3+} ions. Hence too, the intensity of the peaks increase with increase in the Erbium content.

The samples of CdO : Yb, Er give emission in the red region with a slight variation from 626 to 630 nm, which might be due to variation in crystal field. The intensity of the peak increases with increase in the Erbium content. Since these phosphors have not been explored extensively, there is scope for further study.

4.8 References

- [1] Leyu Wang and Yadong Li, “Controlled synthesis and luminescence of lanthanide doped NaYF₄ nanocrystals”, *Chem. Mater.*, 19 (2007), pp. 727-734.
- [2] Z Chao, S Lingdong, Z Yawen and Y Cuhnua, “Rare earth upconversion nanophosphors: synthesis, functionalization and application as biolabels and energy transfer donors”, *J. Rare Earth*, Vol. 28, 6 (2010), pp. 807.
- [3] E. W. Barrera, C. Cascales, M. C. Pujol, J. Carvajal, X. Mateos, M. Aguiló and F. Diaz, “White upconversion luminescence in nanocrystalline (Ho, Tm, Yb):KLuW phosphor”, *Physics Status Solidi*, 8 (2011), pp. 2676-2679.
- [4] G. Liu, X. Chen, “Spectroscopic properties of lanthanides in nanomaterials in Handbook on the physics and chemistry of rare earths”, Vol 37, 2007.
- [5] Jean-Claude G. Bunzli and Svetlana V. Eliseeva, “Basics of lanthanide photophysics” in *Lanthanide Luminescence: Photophysical, analytical, and biological aspects*, Springer Ser Fluorsec, 7 (2011), pp. 1-46.
- [6] W T Carnall, G L Goodman, K Rajnak and R S Rana, “A systematic analysis of the spectra of lanthanides doped into single crystal LaF₃”, *J. Chem. Phys.*, 90 (1989), pp. 3443-3457.
- [7] N. Tyagi, A. A. Reddy and R. Nagarajan, “KLaF₄:Er an efficient upconversion phosphor”, *Optical Materials*, Vol. 33, 1 (2010), pp. 42-47.

- [8] H. Zou, J Li, Q Cao, X Wang, X Hui, Y Li, Y Yu and Xi Yao, “Intensive up-conversion photoluminescence of Er^{3+} doped $\text{Bi}_7\text{Ti}_4\text{NbO}_{21}$ ferroelectric ceramics and its temperature sensing”, *J. Adv. Dielectrics*, Vol. 4, 4 (2014), pp. 1450028-1.
- [9] H. Guo, Y. Qiao, J. Zheng and L Zhao, “Upconversion luminescence of $\text{SrTiO}_3:\text{Er}^{3+}$ ultrafine powders produced by 785 nm laser”, *Chinese J. Chem. Phys.*, Vol. 21, 3 (2008), pp. 233.
- [10] HaiGuo, “Green and red upconversion luminescence in $\text{CeO}_2:\text{Er}^{3+}$ powders produced by 785 nm laser”, *J. Solid State Chem*, 180 (2007), pp. 127-131.
- [11] Yuhu Wang and Junichi Ohwaki, “High-efficiency infrared to visible upconversion of Er^{3+} in BaCl_2 ”, *J. Appl. Phys.*, Vol. 74, 2 (1993), pp. 1272.
- [12] S K Singh, A K Singh, D Kumar, O Prakash and S B Rai, “Efficient UV visible upconversion emission in $\text{Er}^{3+}/\text{Yb}^{3+}$ co-doped La_2O_3 nano crystalline phosphor”, *Appl. Phys. B*, 98 (2010), pp. 173-179.
- [13] W Lu, L Cheng, J Sun, H Zhong, X Li, Y Tian, J Wan, Y Zheng, L Huang, T Yu, H Yu and B Chen, “The concentration effect of upconversion luminescence properties in $\text{Er}^{3+}/\text{Yb}^{3+}$ codoped $\text{Y}_2(\text{MoO}_4)_3$ phosphors”, *Physica B*, 405 (2010), pp. 3284-3288.
- [14] F Wang, D Banerjee, Y Liu, X Chen and X Liu, “Upconversion nanoparticles in biological labeling, imaging and therapy”, *Analyst*, 135 (2010), pp. 1839-1854.
- [15] Chang Sung Lim, “Microwave modified sol gel preparation of $\text{La}_2(\text{MoO}_4)_3:\text{Er}^{3+}/\text{Yb}^{3+}$ particles and their upconversion luminescence properties”, *Analytical Science & Technology*, Vol. 27, 6 (2014), pp. 314-320.

- [16] P Lei, X Liu, L Dong, Z Wang, S Song, X Xu, Y Su, J Feng and H Zhang, “Lanthanide doped Bi₂O₃ upconversion luminescence nanospheres for temperature sensing and optical imaging”, *Dalton Trans.*, 45 (2016), pp. 2686-2693.
- [17] Y Wang and J Ohwaki, “High-efficiency infrared to visible upconversion of Er³⁺ in BaCl₂”, *J. Appl. Phys.*, 74, 2 (1993), pp. 1272.
- [18] HaiGuo, “Green and red upconversion luminescence in CeO₂:Er³⁺ powders produced by 785 nm laser”, *J. Solid State Chem.*, 180 (2007), pp. 127-131.
- [19] Tao Jiang, M Xing, Y Tian, Y Fu, X Yin, H Wang, X Fang and X Luo, “Up-conversion luminescence of Er₂Mo₄O₁₅ under 980 nm and 1550 nm excitation”, *RSC Adv.*, 6 (2016), pp. 109278-109285.
- [20] H Guo, Y Qiao, J Zheng and L Zhao, “Up-conversion luminescence of SrTiO₃:Er³⁺ ultrafine powders produced by 785 nm laser”, *Chin. J. Chem. Phys.*, Vol. 21, 3 (2008), pp. 233-238.
- [21] J H Zeng, T Xie, Z H Li, Y Li, “Monodispersed nanocrystalline fluoropervoskite up-conversion phosphors”, *Crystal growth and Design*, Vol. 7, No. 12 (2007), pp. 2774-2777.
- [22] L Xiong, Z Chen, M Yu, Fu Li, C Liu and C Huang, “Synthesis, characterization and in vivo targeted imaging of amine-functionalized rare-earth up-converting nanophosphors”, *Biomaterials*, 30 (2009), pp. 5592-5600.

- [23] S Jiayue, X Jianbo, Z Xiangyan and DU Haiyan, "Hydrothermal synthesis of $\text{SrF}_2:\text{Yb}^{3+}/\text{Er}^{3+}$ micro/nano crystals with multiform morphologies and upconversion properties", *J. Rare Earth*, Vol. 29, No.1 (2011), pp. 32.
- [24] X Qin, T Yokomori and Y Ju, "Flame synthesis and characterization of rare earth (Er^{3+} , Ho^{3+} and Tm^{3+}) doped upconversionnanophosphors", *Appl. Ply. Lett.*, 90 (2007), pp. 073104 (1-3).
- [25] H Wang and T Nann, "Monodisperseupconversion $\text{GdF}_3:\text{Yb}$, Er rhombi by microwave-assisted synthesis", *Nanoscale Research Letters*, 6 (2011) pp. 267 (1-5).
- [26] S P Hargunani, "Synthesis and upconversion properties of $\text{Er}^{3+}\text{-Yb}^{3+}$ co-doped LiBaBO_3 phosphor", *IARJSET*, Vol.3, 11 (2016), pp. 216.
- [27] M MDobrincic, E Cantelar and F Cusso, "Temporal dynamics of IR-to-visible upconversion in $\text{LiNbO}_3:\text{Er}^{3+}/\text{Yb}^{3+}$: a path to phosphors with tunable chromaticity", *Opt. Mater. Exp.*, Vol. 2, 11 (2012), pp. 1529.
- [28] R Tamrakar, D P Bisen and N Brahme, "Combustion synthesis and upconversion luminescence properties of Er^{3+} , Yb^{3+} doped gadolinium oxide nanophosphor", *Recent Research in Science & Technology*, 4 (8), 2012, pp. 70-72.
- [29] T V Gavrilovic, D J Jovanovic, V Lojpur, A Nikolic and M D Dramicanin, "Influence of $\text{Er}^{3+}/\text{Yb}^{3+}$ concentration ratio on the down conversion and up conversion luminescence and lifetime in $\text{GdVO}_4:\text{Er}^{3+}/\text{Yb}^{3+}$ microcrystals", *Science of Sintering*, 47 (2015), pp. 221-228.

- [30] X Chai, J Li, X Wang, Y Li and Xi Yao, “Color-tunable upconversion photoluminescence and highly performed optical temperature sensing in $\text{Er}^{3+}/\text{Yb}^{3+}$ co-doped ZnWO_4 ”, *Optics Express*, Vol. 24, 20 (2016), pp. 22438.
- [31] H Shen, F Wang, X Fan and M Wang, “Synthesis of $\text{LaF}_3:\text{Yb}^{3+}$, Ln^{3+} nanoparticles with improved upconversion luminescence”, *J. Experimental Nanoscience*, Vol. 2, 4 (2007), pp. 303-311.
- [32] I Hyppanen, J Hosla, J Kankare, M Lastusaari and L Pihlgren, “Up-conversion properties of nanocrystalline $\text{ZrO}_2:\text{Yb}^{3+}$, Er^{3+} phosphors”, *J. Nanomaterials*, 2007, pp.
- [33] G Wang, Q Peng and Y Li, “Upconversion luminescence of monodisperse $\text{CaF}_2:\text{Yb}^{3+}/\text{Er}^{3+}$ nanocrystals”, *J. Am. Chem. Soc.*, 131 (2009), pp. 14200-14201.
- [34] Said Laachir, Mohamed Moussetad, Rahma Adhiri and Ahmed Fahli, “Crystal-Field energy levels of trivalent Erbium ion in cubic symmetry”, *Z. Naturforsch.* 66a, 2011, pp. 457 – 460.